

Impact of climate and land use change on the water resources of a large scale catchment in the Cerrado region, Brazil

Maren Wehling

June 2016

MSc thesis
Master Earth and Environment
Specialization Hydrology and Water Resources
Wageningen University

Acknowledgments

For my thesis research I got the opportunity to stay six months in the beautiful country Brazil. I want to thank everybody who supported me during that time.

First of all I want to thank my parents for giving me the opportunity to go to Brazil and my fiancé Cornelis Dingemanse for supporting me in the decision to go abroad and for his technical support with ArcGIS.

A special thanks goes to my supervisors from Wageningen University, Roel Dijkema and Jos van Dam, for bringing me in contact with Lineu Rodrigues and for their support and feedback during my research. Furthermore I want to thank Claudia Brauer from Wageningen University for answering all my questions about R. I want to thank Bas Agerbeek for the nice moments we had together in Brasília.

I want to thank Vitor and his family for giving me a nice place to stay during the six months and for bringing me in contact with his friends, which makes me feel at home very soon. I want to thank Lucas and Winie and all other people I met in Brasília for making the six months in Brazil to one of the greatest times of my life.

I want to thank Fernando Falco Pruski and the University of Viçosa, who made it possible for me to stay in Brazil to do my research for so many months. I also want to thank Jose Roberto Rodrigues Peres who gave me the opportunity to carry out my research at the EMBRAPA research institute. Furthermore I want to thank Raquel and Nickolas for helping me during my time at EMBRAPA. At EMBRAPA I also met Gabriela, who I want to thank taking me to work a lot of times and introducing me to her family.

Last but not least I want to thank my supervisor in Brazil: Lineu Neiva Rodrigues. He gave me the opportunity to come to Brazil and carry out my thesis research at EMBRAPA. He supported me with good feedback and helped me collecting my data. Next to being a good supervisor he also helped me with the logistics to come to Brazil and introduced me to his lovely family. I spent the Christmas holidays and some evenings with his family which gave me the opportunity to experience real Brazilian family life. During my six months in Brazil Lineu and his family became good friends. Thank you very much again for giving me this big opportunity to experience so many things. A time I will never forget in my life.

Maren Wehling

Arnhem, 17th June 2016

Summary

World fresh water resources are limited and the fresh water demand will even increase in future due to a growth in population and expansion of irrigated agriculture. At the same time land use change and climate change are expected, which will lead to a decrease in available water. For Brazil it is of great importance to analyze the possible effects of these changes, as they are holding 12% of worlds fresh water and with irrigated agriculture as the largest water user. Especially for the Paracatu River Basin, where many agricultural areas are located, this analysis is important to plan future water management. The aim of this research is to analyze the impact of climate and land use change and irrigation on the (surface) water resources of the Paracatu River Basin.

The Paracatu River Basin is a tributary of the São Francisco River with a total drainage area of 45600km². The climate of the PRB is tropical with a wet season between October and April and a dry season between May and September. The annual average rainfall is 1338mm. The Paracatu River is responsible for 24% of the flow of the São Francisco River, with a monthly average discharge between 200 and 1000m³/sec. The land use of the Paracatu River Basin is mainly savanna which was decreased significantly during the last 30 years.

To analyze climate and land use change a hydrological model was used. For this research SWAT (Soil Water Assessment Tool) was chosen. It is a physically based model with its major components climate, hydrology, soil properties and land use. After editing the data as input data and calibration of the model, a scenario analysis was carried out.

For the climate change scenarios results of two regional models based on two global climate models were used: ETA HadGEM2-ES and ETA-MIROC5. For both climate models two representative concentration pathways were used: rcp4.5 and rcp8.5. The time series per climate model, pathway and climate parameter were corrected with two methods: The BIAS-correction- and the DELTA-method. This resulted in eight different input data sets for each climate parameter (precipitation, temperature, solar radiation, relative humidity and wind speed). The calibrated model was tested with these datasets. The input time series of the rcp8.5 pathway resulted in larger decreases in discharge compared to the rcp4.5 scenarios. Furthermore the decrease in discharge is larger for the ETA HadGEM2-ES scenarios compared to the ETA-MIROC5 scenarios. The main reason for decrease in discharge for all scenarios is a decrease in rainfall. The decrease in discharge differs between 20 and 95% dependent on the used climate model, pathway, correction method and future period.

For analyzing land use change the results of the model with the 1984 land use map were compared to the results of the 2013 land use map. Afterwards five future scenario's were analyzed by increasing rain-fed agriculture and decreasing pasture with 20 and 30%, savanna with 20 and 30% and decreasing savanna and pasture at the same time with resp. 20 and 30%. The impact of land use change is smaller than the impact of climate change, as the decrease in discharge is less.

The impact of irrigation on the water resources was analyzed by comparing the observed discharge of 1984/1985 (nearly no irrigation) with the discharge values of 2010/2011 (irrigation area 60 times as big as in 1984). The decrease in discharge is assumed to be caused by irrigation only. The average decrease in discharge is 253m³/sec. Afterwards the irrigation area is increased with 10, 20, 30, 50 and 100%. The discharge decreases continuously when increasing the irrigated area. When the area is increased by 50 and 100% the discharge becomes zero during some months of the dry period. For future water management this has to be taken into account.

All in all climate change is of larger influence on the water resources of the Paracatu River Basin than land use change. Increase in irrigation can lead to a no-flow situation during the dry season and a critical situation for the river.

Keywords: ArcSWAT, Paracatu River Basin, Climate change, Land use change, Irrigation

Contents

Acknowledgements	iii
Summary	v
1 Introduction	1
1.1 Problem analysis	1
1.2 Research objectives	1
1.3 Research questions	1
1.4 Thesis contents	2
2 Project Area	3
2.1 Location	3
2.2 Topography	3
2.3 Soil	3
2.4 Geology	4
2.5 Climate	4
2.6 Hydrological characteristics	4
2.7 Landuse	6
2.8 Irrigation	6
2.8.1 Irrigation in current situation	7
2.8.2 Development of irrigation in the past	7
3 Scenarios	9
3.1 Climate change scenario's	9
3.1.1 Climate models	9
3.1.2 Representative concentration pathways	9
3.2 Land use change scenario's	10
3.3 Irrigation scenario's	10
4 Method	11
4.1 Field visits	11
4.2 Hydrological Modeling	11
4.2.1 Model choice	11
4.2.2 Soil Water Assessment Tool - SWAT	11
4.3 Data analysis and editing	15
4.3.1 General data	15
4.3.2 Hydrological data	15
4.3.3 Meteorological data	16
4.3.4 Land use and soil data	17
4.3.5 Climate and land use change data	17
5 Results	21
5.1 Current discharge characteristics	21
5.2 Impact of climate change on water resources	21

5.2.1	ETA HadGEM2-ES	21
5.2.2	ETA MIROC 5	23
5.2.3	Summary of the climate change results	23
5.3	Impact of land use change on water resources	24
5.4	Impact of irrigation on water resources	24
6	Discussion and Conclusion	25
6.1	Discussion and Recommendations	25
6.1.1	Data	25
6.1.2	Hydrologic modelling and calibration	25
6.1.3	Climate Change Scenarios	25
6.1.4	Land use Change Scenarios	25
6.1.5	Irrigation Scenario's	25
6.2	Conclusion	26
	Bibliography	27
	A Report field visit	31
	B Locations weather and discharge stations	33
	C Data editing	37
	D Climate change input	39
	E Climate change results	45
	F Maps and figures	49

List of Figures

1.1	Location of Paracatu River Basin	2
2.1	Digital Elevation Map of the Paracatu River Basin	3
2.2	Soilmap of the Paracatu River Basin, based on the soil maps of the IBGE database (IBGE, 2016) and Mingoti et al. (2015).	3
2.3	Main geological units of Upper Paracatu River (Mulholland et al., 2012)	5
2.4	Monthly average rainfall and potential evapotranspiration	5
2.5	Average rainfall per month for different rainfall stations within the PRB, based on data provided by ANA (National Water Agency)	5
2.6	Average rainfall per day for the Cachoeira do Predao rainfall station	6
2.7	Monthly averages of different meteorological parameters: relative humidity, solar radiation, maximum and minimum temperature, wind speed	6
2.8	Sub basins and main streams of Paracatu River Basin, based on the maps of ANA (National Water Agency) and Rodriguez (2004)	7
2.9	Average discharge and rainfall for measurement stations most downstream of the Paracatu River and downstream of the PRB outlet	7
2.10	Landuse change of the past 30 years	8
2.11	Change in land use from 1984 to 2013	8
2.12	Development of irrigated areas within the Preto River Basin of the last 30 years	8
3.1	Trends in radiative forcing for different RCPs, (Van Vuuren et al., 2011), blue = rcp8.5, black = rcp6, red = rcp4.5, green = rcp2.6	9
4.1	Example of the SWAT check inside ArcSWAT, developed by White et al. (2014)	13
4.2	Baserun, calibration run and validation run compared to the observed values	14
4.3	Radiation data provided by NASA compared to transformed radiation based on sunshine hours	17
4.4	Ratio of discharge and precipitation, based on monthly averages	19
4.5	Determination of decrease in discharge due to irrigation	20
5.1	Monthly averages (1984-1986) of observed and simulated discharge at Porto Alegre station	21
5.2	Flow duration curve, Porto Alegre, 1984-1986	21
5.3	Monthly averages for different climate scenario's (ETA-model) at the Porto Alegre station	22
5.4	Monthly averages for different climate scenario's (MIROC-model) at the Porto Alegre station	23
5.5	Monthly averages for different land use change scenario's at the Porto Alegre station	24
5.6	Monthly averages for different irrigation scenario's at the Porto Alegre station	24
A.1	Paracatu River	31
A.2	Buriti Vermelho River	32
B.1	Locations chosen rainfall stations inside and outside the PRB	34
B.2	Locations chosen meteorological stations inside and outside the PRB	35
B.3	Location discharge stations inside and outside the PRB	36
D.1	Climate change input - Precipitation - ETA-model	39
D.2	Climate change input - Precipitation - MIROC-model	39

D.3	Climate change input - Temperature - ETA-model	40
D.4	Climate change input - Temperature - MIROC-model	40
D.5	Climate change input - Solar Radiation - ETA-model	41
D.6	Climate change input - Solar Radiation - MIROC-model	41
D.7	Climate change input - Wind speed - ETA-model	42
D.8	Climate change input - Wind speed - MIROC-model	42
D.9	Climate change input - Relative Humidity - ETA-model	43
D.10	Climate change input - Relative Humidity - MIROC-model	43
F.1	Digital Elevation Map of the Paracatu River Basin	50
F.2	Soilmap of the Paracatu River Basin, based on the soil maps of the IBGE database (IBGE, 2016) and Mingoti et al. (2015).	51
F.3	Main geological units of Upper Paracatu River (Mulholland et al., 2012)	52
F.4	Sub basins and main streams of Paracatu River Basin, based on the maps of ANA (National Water Agency) and Rodriguez (2004)	53
F.5	Landuse change of the past 30 years	54
F.6	Development of irrigated areas within the Preto River Basin of the last 30 years	55

List of Tables

3.1	Future land use change scenario's	10
4.1	Calibration parameters and their values before and after calibration, source of the definitions: Arnold et al. (2012a)	13
C.1	Used data and data sources	38
E.1	Summary results ETA HadGEM2-ES scenario's	46
E.2	Summary results ETA MIROC5 scenario's	47

1 | Introduction

1.1 Problem analysis

World wide the fresh water resources are limited and the fresh water demand will even increase in future, because of a global expansion of irrigated agriculture with up to 30% by 2030 (according to the Food and Agricultural Organization - FAO, Bof et al. (2013)). At the same time climate and land use change will have influence on the water resources. Land use change, e.g. the expansion of agricultural areas, may lead to higher water demands, but can also have impact on other key elements of the hydrological cycle, like evapotranspiration, precipitation and surface temperature (Stonestrom et al., 2009). Climate change can lead to an decrease in water availability, because of changes in temperature, precipitation amount and -patterns.

Brazil holds 12% of worlds fresh water. Irrigated agriculture is, like in most of the countries, the largest water user with nearly 70% of Brazilians water use (Braga et al., 2009). If the irrigated areas will expand, this water demand can get even higher and lead to conflicts with other water users. Furthermore decreases in rainfall and increases in temperature can be expected according to IPCC (2014). The reduction of precipitation can lead to water shortages and decreases the productivity of the agricultural sector. Therefore it is important to get a good impression of available water resources and the impacts, climate and land use change will have on them.

This is also of great importance for the Paracatu River Basin (PRB), since irrigated agriculture takes place within the PRB and will increase in future (see figure 1.1 for the location of the Paracatu River Basin). The Paracatu River is one of the most important tributaries of the São-Francisco river and therefore it is also essential to make sure that the water supply from the Paracatu River to the São-Francisco river is guaranteed. Furthermore some tributaries of the PRB are already in an alert situation, with respect to the ratio between water demand and water availability (Braga et al., 2009). In some parts of the PRB conflicts about water use have already occurred, between different users of irrigation systems and also between them and other water users (Bilibio et al., 2011). Due to climate and land use change the number of tributaries in an alert situation could increase and lead to even more conflicts between different water users and to a reduced water supply to the São-Francisco river.

Impacts of climate change on the water resources of the PRB were recently analyzed by Mello et al. (2008), but not in combination with land use change. Furthermore it is not yet analyzed how large the influence of irrigation is on the water resources of the PRB. Therefore research is necessary in which the components climate change, land use change and irrigation are combined to give a good impression of possible challenges of future water management within the PRB.

1.2 Research objectives

Based on the problem description above three research objectives are formulated. The first aim is to get a clear impression of the current situation within the PRB, regarding the water resources. Therefore a determination of the current surface water availability of the PRB is necessary, as well as an analysis of the current influence of irrigated agriculture on the water resources of the PRB. The second aim is to investigate the impact of climate and land use change on the water resources of the PRB over 50 years, based on a scenario analysis. The last aim is to analyze the effects of a changing water availability on irrigation.

1.3 Research questions

The research objectives lead to the following main question:

What is the impact of climate and land use change on the (surface) water resources of the Paracatu River Basin and how large is the impact of irrigated agriculture?

To answer this question, the following sub-questions needs to be answered.

1. *What are the current discharge characteristics of the Paracatu River Basin?*
2. *Which climate and land use change is expected in the next 50 years ?*
3. *How will the discharge of the Paracatu River and therefore the (surface) water availability change in future based on expected climate and land use change?*
4. *How large is the impact of irrigation on the water availability of the PRB now and in the future?*

Location Paracatu River Basin

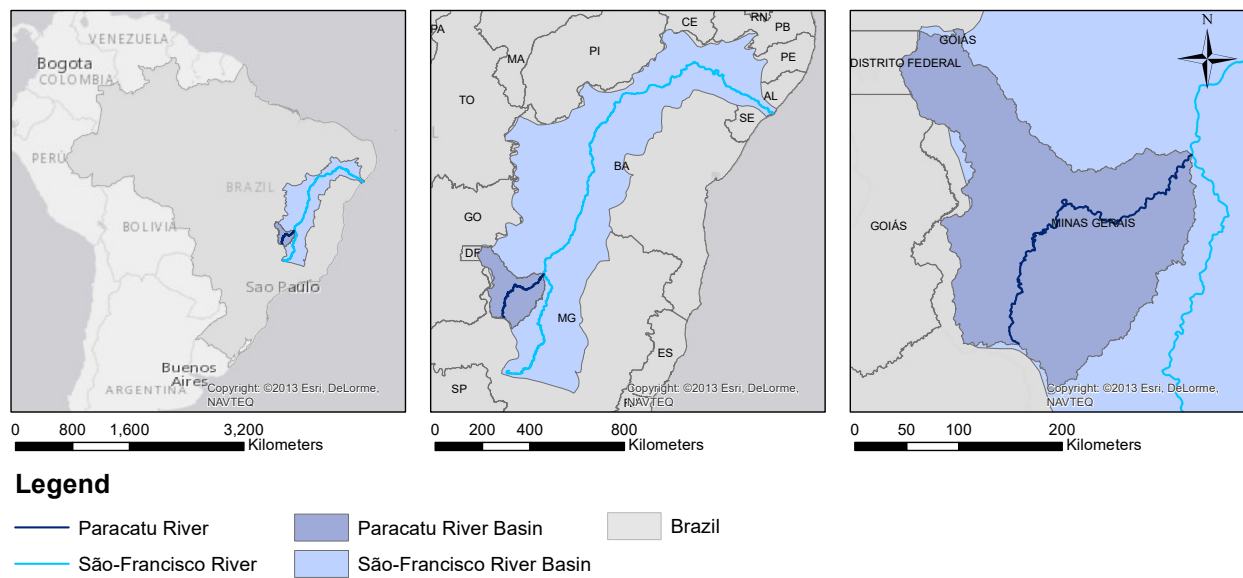


Figure 1.1: Location of Paracatu River Basin

1.4 Thesis contents

In chapter 2 a study site description is given, including information about soil, the hydrological system and on how the land use has changed from 1984 until now. In chapter 3 the scenario's are described. The following chapter describes the used method, which contains three main activities: Literature study, data analysis and Hydrological modeling. Chapter 5 describes the results of the scenario analysis of irrigation, climate- and land use change. The discussion and conclusions can be found in chapter 6. All maps can be found in a bigger format in appendix F.

2 | Project Area

2.1 Location

The Paracatu River Basin (PRB) is located in the Medium São-Francisco region (see figure 1.1) of Brazil. The Paracatu River drains areas from the states of Minas Geiras, Goiás and Federal District with a total drainage area of ca. 45600 km². (Fujaco and Leite, 2010; Mulholland et al., 2012). The Paracatu River Basin is the second largest sub-basin of the São-Francisco River Basin. It is one of the most important tributaries of the São-Francisco River, being responsible for 24% of the flow.

2.2 Topography

The Paracatu River Basin is located at a height between 440 and 1190 MASL (see figure 2.1). The lowest parts of the basin can be found close to the Paracatu River. The highest parts are located in the northwest in the upstream area of the Preto River Basin and in the south east of the PRB.

Digital Elevation Map of the Paracatu River Basin

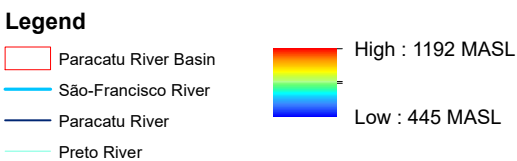
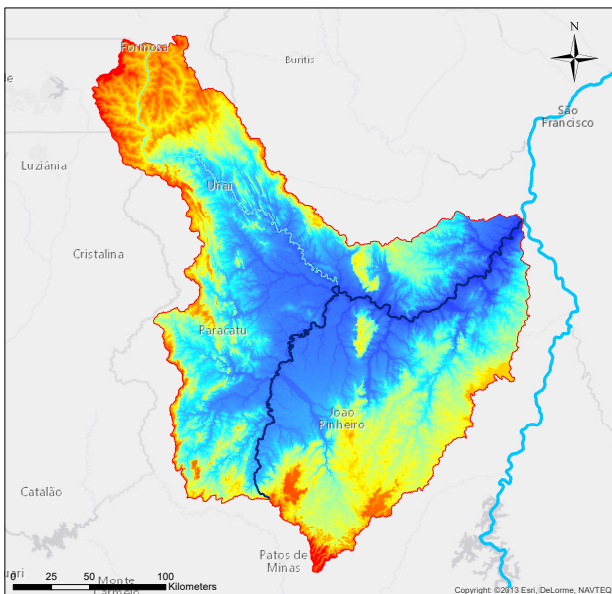


Figure 2.1: Digital Elevation Map of the Paracatu River Basin

2.3 Soil

Within the Paracatu River Basin different soil types can be found, see figure 2.2. The soil class which covers most of the area is Oxisols (Latosols). The two types of oxisols, which can be found most in the project area are Red Oxisols and Red-Yellow Oxisols. Furthermore Cambisols and Lithosol covers larger areas of the basin. In the areas around the river alluvial soil can be found. Other types of soil within the area, which just cover small parts are different types of Neosols (Fluvic, Litholic and Quartzarenic), stony outcrop, Plinthosols, Petroplinthosols, hydromorphic indiscriminate soil, Red Utisols, Gleysols, Quartz sand, Red-Yellow and Dark-Red Podzolic.

Soil Map of the Paracatu River Basin

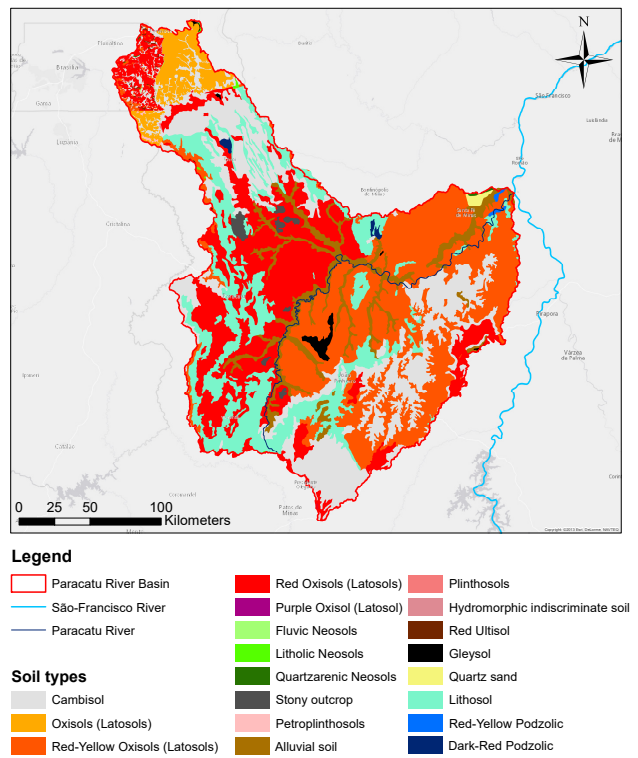


Figure 2.2: Soilmap of the Paracatu River Basin, based on the soil maps of the IBGE database (IBGE, 2016) and Mingoti et al. (2015).

According to Aquino et al. (2013) most of these soil types have a relatively high clay content (medium to very clayey). The soil parameters based on Mingoti et al. (2015) show that the clay content of the first layer is highest for Purple Lathosol, alluvial soil and Fluvic Neosol

and lowest for (Red) Lathosol and Lithosol. Purple Lathosol and Gleysol have the highest clay content in the second layer. The soil types with the lowest clay content in the second layer are quartz sand, Quartzarenic Neosol, Hydromorphic indiscriminate soil and Lithosol. Because of their dystrophic character most of the soils have a base saturation percentage lower than 50% (Lau, 2016) and are mainly medium to low fertility soils. Furthermore Lau (2016) defines Latosols as very deep, very well drained homogenous highly weathered and leached soils with medium to very high clay content.

2.4 Geology

A large part of the Paracatu Basin is located within the geological units of the Vazante and Canasta Groups in the Brasília Fold Belt (see figure 2.3). While the metasediments of the Vazante Group mainly consist of a clayey and dolomitic clayey stromatolite sequence, the Canasta Group sediments are composed of siliciclastic metasedimentary rocks. These rocks consist of carbonaceous phyllite layers (Paracatu Formation) and are covered by sericitic and chloritic phyllites, as well as quartzites. (Mullolland et al., 2012)

2.5 Climate

The climate in the Paracatu River Basin is predominantly tropical wet with an annual average rainfall of 1338mm. The rainy period lasts from October to April with 93% of the total annual rainfall falling during these months. Within the rainy period, November, December and January are the wettest months. The annual average evapotranspiration amounts 1140mm and the annual average temperature lies between 22-24°C. (Vasconcelos et al., 2013; Lima et al., 2012). Typical for the region, in which the project area is located, is a combination of high evapotranspiration and low rainfall during the dry season (FAO, 2016) (see also figure 2.4).

In figure 2.5 the monthly average rainfall of the chosen rainfall stations inside the PRB are shown (see appendix B for the locations of the rainfall and meteorological stations). The yearly distribution is clearly visible with the highest measured values of above 200mm/month between November and January and values around 0mm during the driest months June, July and August. Remarkable is the decrease in precipitation from between December and January and the kink in February, all stations have. This is caused by a three weeks lasting dry period, called "veranico", which usually lasts from mid January to begin February (Brito et al., 2003). Actually this dry season is shifted in time in the

study area and starts at the end of January and lasts until mid to end February (see figure 2.6). Therefore the influence of the dry season is larger in February.

In figure 2.7 the monthly averages of four meteorological parameters are shown: relative humidity, solar radiation, minimum and maximum temperature and wind speed. The monthly averages of the relative humidity in the study area are between 55 and 80%. The relative humidity is lowest in August and September, because it is the end of the dry season. The highest value is measured in December, which is one of the wettest months of the rainy period. In the graph a kink can be seen around February, which is caused by the dry period "veranico".

Solar radiation has monthly averages between 16 and 20 MJ/m². The lowest values are measured during the first months of the dry period (May, June and July). and the highest values in February and October. The temperature graphs follow a similar pattern, because temperature is strongly influenced by solar radiation. The monthly averages differs between 27 and 31°C for maximum temperature (T_{max}) and 13 and 19°C for minimum temperature (T_{min}). The monthly averages for wind speed differ between 0.95 and 1.3 m/sec. The highest averages can be found between July and October and the lowest values in March and May.

2.6 Hydrological characteristics

The São Francisco River has 36 tributaries of which 19 are perennial. The Paracatu River belongs to these 19 perennial tributaries (Pereira et al., 2007) and is furthermore one of the non-regulated tributaries of the São Francisco River (de Andrade e Santos et al., 2012).

The Paracatu River flows from South to the North-East into the São-Francisco river. It is fed by several smaller rivers and streams. The main streams are determined based on the thesis of Rodriguez (2004) and the data provided by ANA. Furthermore the Paracatu River Basin can be divided into several sub basins, which names are based on the mainstreams. These sub basins are the natural sub basins, provided by ANA and are not the ones used within the hydrological model. The sub basins in the model are based on the locations of the discharge measurement stations and the digital elevation map. Therefore the amount of sub basins in the model is larger and the locations can differ. The mainstreams, as well as the natural sub basins are shown in figure 2.8.

In figure 2.9 the average discharges for each month, measured at the Porto Alegre station (the most down-

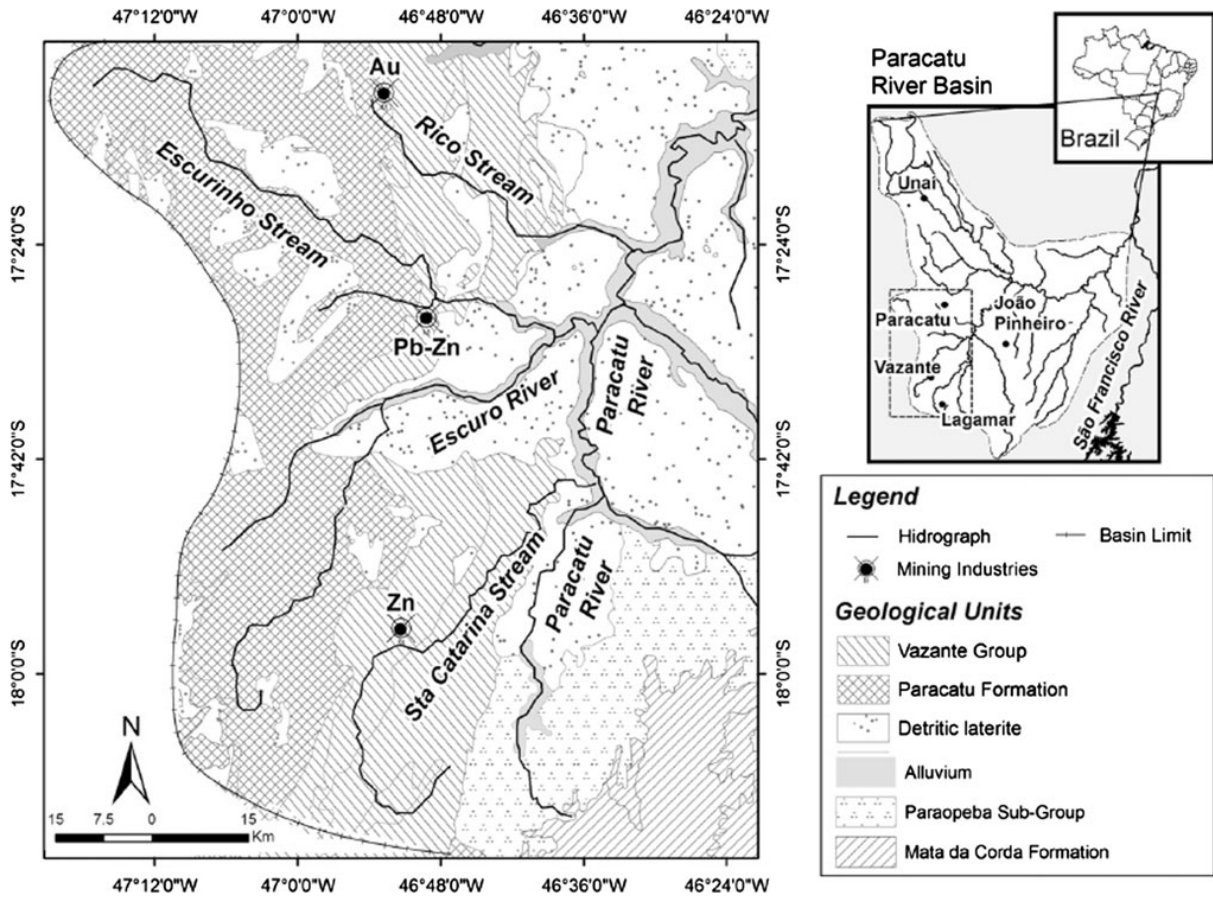


Figure 2.3: Main geological units of Upper Paracatu River (Mulholland et al., 2012)

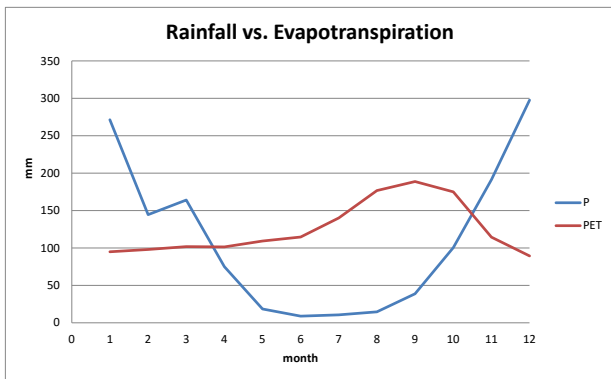


Figure 2.4: Monthly average rainfall and potential evapotranspiration

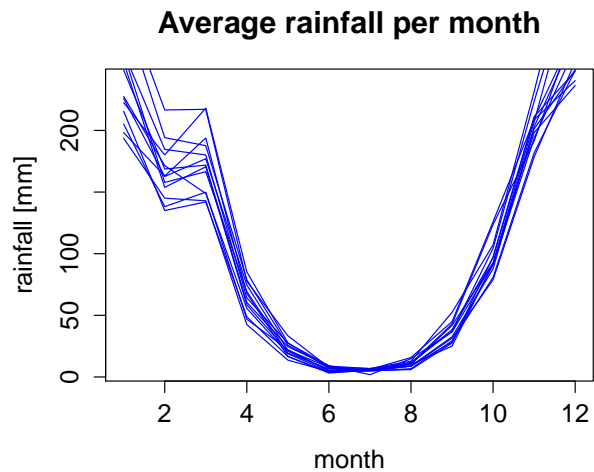


Figure 2.5: Average rainfall per month for different rainfall stations within the PRB, based on data provided by ANA (National Water Agency)

stream discharge measurement station), respectively at the São Romão station (just outside the PRB basin) are shown (see stations 13 and 22 in figure B.3, appendix B). At both stations the highest average discharge is measured in January with ca. 940m³/sec, respectively 3160m³/sec. The lowest average values are recorded at the end of the dry season in September with 140m³/sec at the Porto Alegre station and 740m³/sec at São Romão

station. The monthly rainfall sums are averaged as well for precipitation stations near the stream gauge stations. The average rainfall values follow a similar pattern like the discharge values, with the lowest values during the

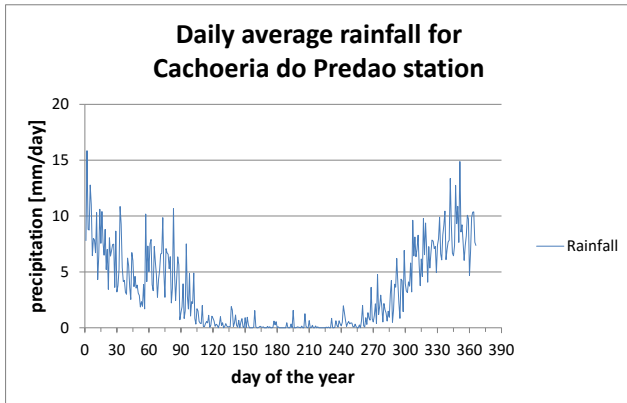


Figure 2.6: Average rainfall per day for the Cachoeira do Predao rainfall station

dry period and highest values in December. The similar patterns confirm, that the main source of discharge in the Paracatu River is orographic precipitation (Biswas et al., 1999). The kink in the first graph (Figure 2.9,a) around February is caused by the dry period "veranico".

2.7 Landuse

The land use maps (see figure 2.10) were created based on LandSat images. They give a good impression of how the land use has changed within the last 30 years. In 1984 the main land use within the project area was 'Savannah' with nearly 80% of the total area, followed by 'Pasture' with ca. 9%. The area of 'Agriculture' (rainfed) and 'Forest' were nearly the same in 1984 with ca.6% each. There were only small areas of irrigated agriculture (0.04% of total area) and even smaller mining areas (0.01%).

From 1984 to 2013 there was a slightly increase of the urban and mining areas and a slightly decrease of the forest areas (see figure 2.11). More important is the big increase in pasture, from 9% to 32% . At the same time the savannah areas decreased from 80% to 51%. This is in agreement with De Oliveira Latuf et al. (2007), who states that there was a significant decrease of the savannah areas in the Preto and Entre RIBEIROS sub basin between 1985 and 2000. According to them this decrease was mainly caused by the cultivation of these areas. There is no increase in rain-fed agriculture, but the area of irrigated agriculture in 2013 is nearly 60 times as big as in 1984 (from 21km² to more nearly 1200km²). The main crops in the region are beans, corn and soybean (Rodriguez, 2004).

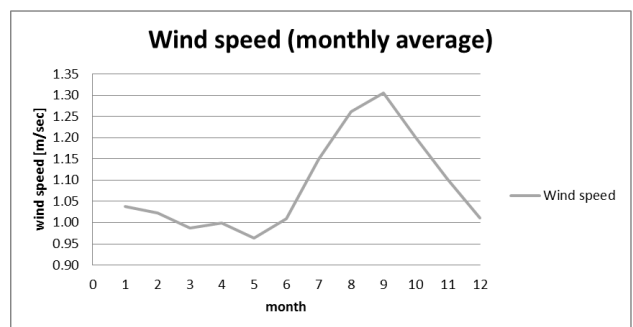
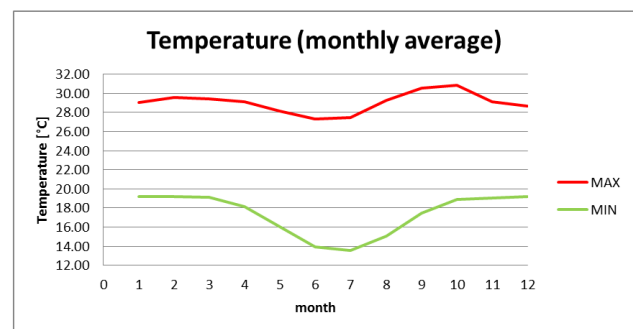
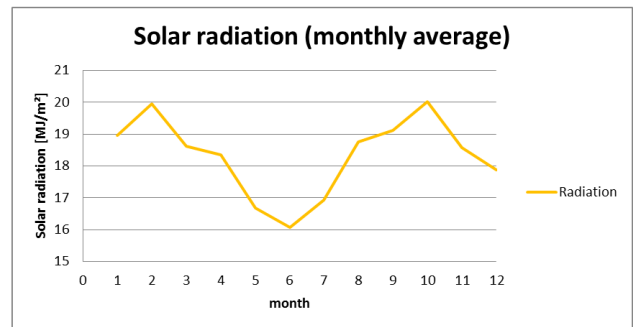
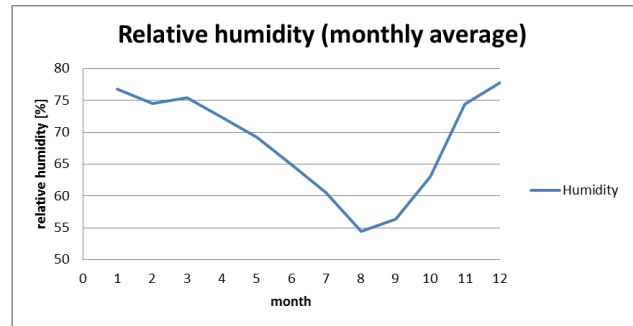
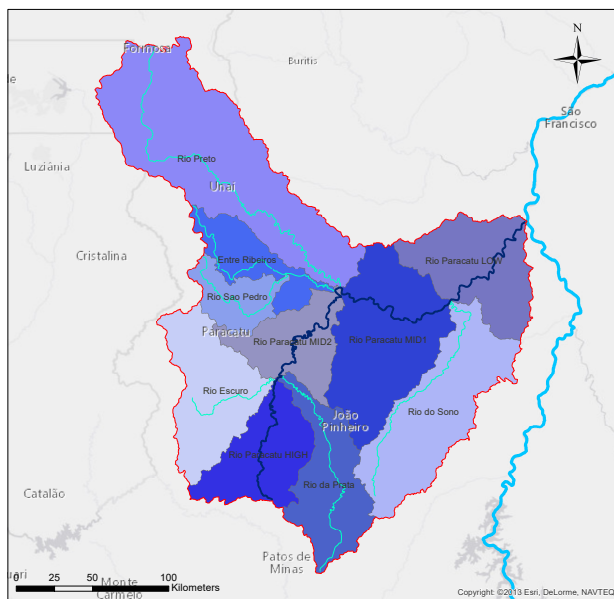


Figure 2.7: Monthly averages of different meteorological parameters: relative humidity, solar radiation, maximum and minimum temperature, wind speed

2.8 Irrigation

In this paragraph the development of irrigated areas in the last 30 years is discussed, as well as the irrigation in the current situation. Thereby the size of the irrigated areas and the used irrigation methods are analyzed.

Subbasins and main streams of the PRB



Legend

- ▭ Paracatu River Basin
- ▭ São-Francisco River
- ▭ Paracatu River
- ▭ Main streams Paracatu

Figure 2.8: Sub basins and main streams of Paracatu River Basin, based on the maps of ANA (National Water Agency) and Rodriguez (2004)

2.8.1 Irrigation in current situation

The most used irrigation method within the Paracatu River Basin is center pivot irrigation. The total irrigated area of the Paracatu River Basin in 2013 had a size of nearly 120000 ha, which is more than 2% of the total basin (ca. 4.5 M ha) (see figure 2.10). With diameters between 180 and 1900m the areas irrigated by one center pivot differ between 2.5 and nearly 300ha. The annual average water withdrawal by irrigation in 1996 was 0.15L/s per ha and for the month with the highest demand the water withdrawal was 0.34 L/s per ha (Rodríguez et al., 2007). No data is found about specific values of current withdrawal. It is assumed that the water withdrawal per ha is the same, but that the total withdrawal increased, because of the increasing irrigation areas.

2.8.2 Development of irrigation in the past

The Preto River basin is used as an example to show how the irrigated areas have been expanded in the last 30 years (see figure 2.12). Because center pivot irrigation is the most used irrigation technique within the study area, only the increase in center pivot irrigation is analyzed. While in 1984 there was nearly no irrigation (only 590 ha irri-

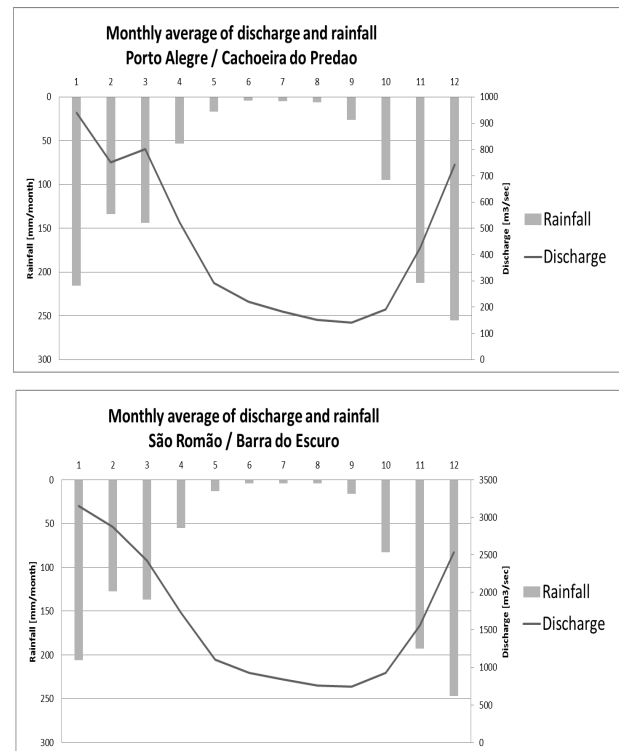


Figure 2.9: Average discharge and rainfall for measurement stations most downstream of the Paracatu River and downstream of the PRB outlet

gated of a total area of nearly 972000 ha), the irrigation areas increased nearly ten times by 1989. The smallest absolute increase took place between 1994 and 1999 (ca. 2070 ha), while the biggest absolute increase took place between 2009 and 2014 (ca. 10680 ha). The total increase between 1984 and 2014 was more than 35000 ha. According to FAO (2016) the potential for irrigation in the cerrado regions has increased significantly during the last years, due to advances in soil management and irrigation techniques.

Land use change from 1984 to 2013

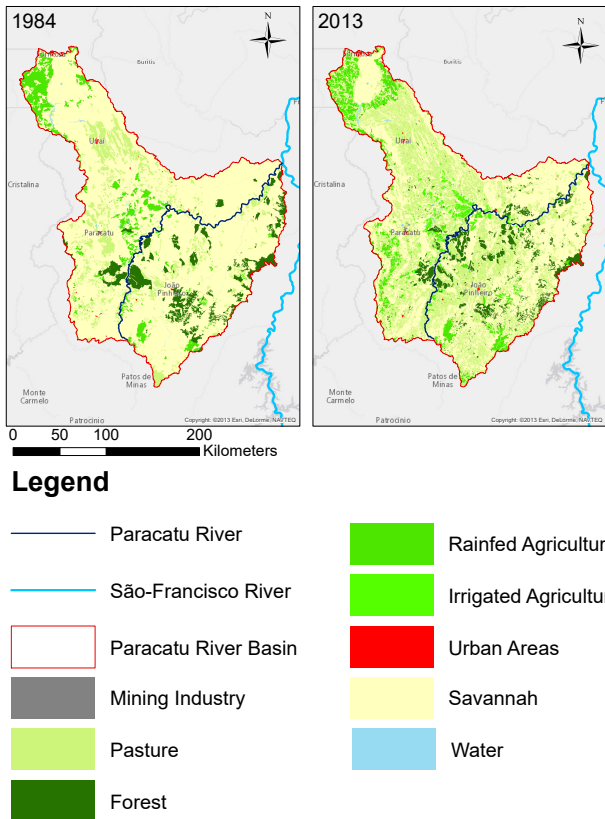


Figure 2.10: Landuse change of the past 30 years

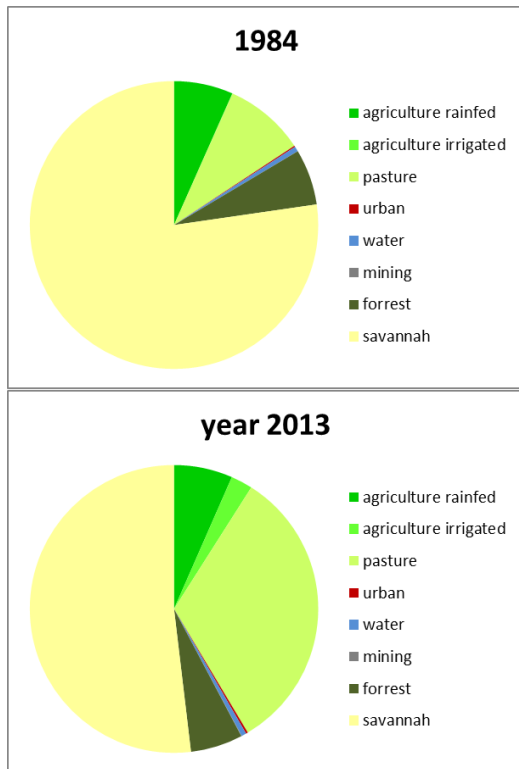


Figure 2.11: Change in land use from 1984 to 2013

Development of Irrigation (Center-pivot)

Preto River Basin from 1984 to 2014

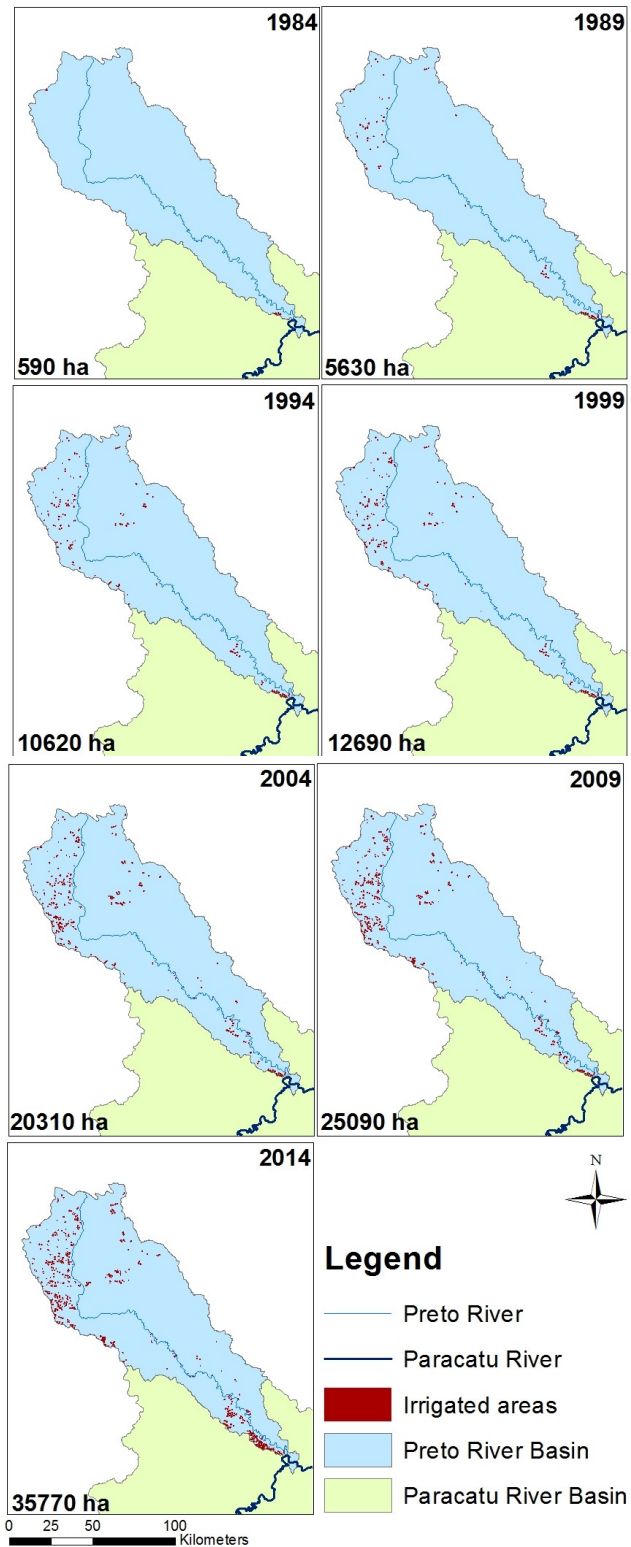


Figure 2.12: Development of irrigated areas within the Preto River Basin of the last 30 years

3 | Scenarios

3.1 Climate change scenario's

The climate is changing and will change even more in future. Therefore it is important to take climate change into account for future water management. To analyze climate change, climate change scenario's are necessary. The aim of these scenario's is "a plausible representation of future climate that has been constructed for explicit use in investigating the potential impacts of anthropogenic climate change" (Mearns et al., 2001). There are different methods to create these scenario's like climate modeling, temporal and spatial analogues and expert judgment (Mearns et al., 2001). According to IPCC (2014) climate modeling can be a very useful tool to create different future climate scenario's with various forcings.

Therefore it is chosen to create climate scenario's using two regional climate models based on the global models ETA HadGEM2-ES and ETA MIROC 5. It is chosen to use these two regional models, because climate change data is available for all required climate parameters and are more detailed than global climate models. The results of both models are provided by INPE (Instituto Nacional de Pesquisas Espaciais), a national research institute of Brazil. Per model two representative concentration pathways, adapted in the 5th Assessment report of IPCC (IPCC, 2014), are used: RCP 4.5 and RCP 8.5. The models, as well as the pathways are described in more detail below.

3.1.1 Climate models

Both models used in this research are regional models of INPE, based on two global climate models. The two global models are HadGEM2-ES and ETA-MIROC5. The HadGEM2-ES model is developed by the Hadley centre and has a resolution of 1.875 degrees (longitude) and 1.275 degrees (latitude), as well as 38 levels in the atmosphere. The vegetation scheme of the model is dynamic with a carbon cycle presentation.(Chou et al., 2014) The MIROC5-model is described by Chou et al. (2014) as a coupled ocean-atmosphere model with a resolution of 150km horizontal and 40 levels in vertical direction. The MIROC5-model is developed in Japan. The regional models based on those global models have a resolution of approximately 20m.

3.1.2 Representative concentration pathways

The representative concentration pathways (RCPs) are pathways of radiative forcing and not detailed socio-economic scenario's (Penalba and Rivera, 2013). Radiative forcing can be defined as "additional energy taken up by the Earth System due to the enhanced greenhouse effect" or as the "difference in the balance of energy that enters atmosphere and the amount that is returned to space compared to the pre-industrial situation" (Bjornaes, 2015). When the radiative forcing increases, the global temperature rises as well, but the exact relationship is not known yet.

There are four pathways developed by different institutions: RCP 2.6, RCP 4.5, RCP 6.0 and RCP 8.5. Because these pathways were developed, using different and independent models, they cannot be compared directly (Bjornaes, 2015). The number in the name of the pathways stands for the radiative forcing reached within the pathway, e.g. for RCP 8.5 the radiative forcing would be 8.5 W/m² by 2100 (see figure 3.1). Within this research only two of the four representative concentration pathways are analyzed: RCP4.5 and RCP8.5. They are described in more detail below.

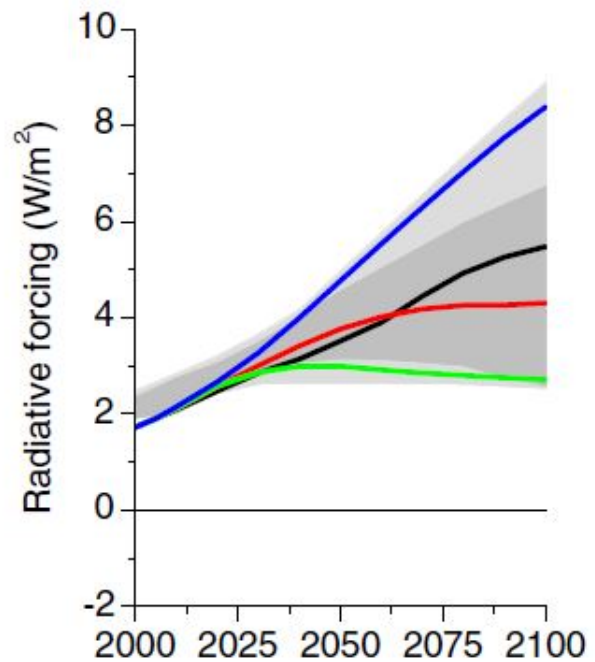


Figure 3.1: Trends in radiative forcing for different RCPs, (Van Vuuren et al., 2011), blue = rcp8.5, black = rcp6, red = rcp4.5, green = rcp2.6

RCP 8.5

The RCP 8.5 is a high emission pathway that is developed by the International Institute for Applied System Analysis in Austria (IIASA). For this pathway it is assumed that there are no policy changes to reduce emissions and therefore the greenhouse gas concentration will increase to a high amount in future. Other assumptions according to Bjornaes (2015) are:

- "Three times today's CO₂ - emission by 2100
- rapid increase in methane emissions
- increased use of croplands and grassland which is driven by an increase in population
- a world population of 12 billion by 2100
- lower rate of technology development
- heavy reliance on fossil fuels
- high energy intensity
- no implementation of climate policies"

RCP 4.5

According to Bjornaes (2015) the RCP 4.5 is an intermediate emission pathway, developed by the Pacific Northwest National Laboratory in the USA. It is similar to the SRES scenario B1. This pathway predict a stabilization of the radiative forcing shortly after 2100. Bjornaes (2015) other assumptions about this pathway are:

- "lower energy intensity
- strong reforestation programs
- decreasing use of croplands and grasslands due to yield increases and dietary changes
- stringent climate policies
- stable methane emissions
- CO₂ - emissions increase only slightly before decline commences around 2040"

3.2 Land use change scenario's

Like described in chapter 2 the land use has changed in the past years. According to Lorz et al. (2012) the biggest change in land use was the increase in agricultural areas with a decrease of the savanna areas. Therefore the scenario's will concentrate on this type of land use change. To analyze land use change, different land use change scenario's are simulated. The first scenario is a historical scenario, analyzing the change between 1984 and 2013. Therefore the land use map of 2013 is used (see figure 2.10, chapter 2). In the past pasture and irrigated agriculture increased, while savanna decreased. For the future, further increase in agriculture is expected. The increase

in agriculture will lead to a decrease of savanna, following the trend of the past. Also an decrease in pasture can be expected, as the area increased a lot during the last years. These areas might turn into rain-fed agriculture in the future. To analyze the impact of a decrease in pasture, resp. savanna while rain-fed agriculture is increasing, five future scenario's are analyzed (see table 3.1).

Table 3.1: Future land use change scenario's

Scenario	Decrease Pasture	Decrease Savanna	Increase rain-fed agriculture
Future 1	20%	0%	99%
Future 2	40%	0%	198%
Future 3	0%	20%	158%
Future 4	0%	40%	316%
Future 5	30%	20%	307%

3.3 Irrigation scenario's

The irrigated areas of 2013 are nearly 60 times as big as in 1984 (from 21km² to nearly 1200km²), when there was nearly no irrigation (see chapter 2). For the future a further increase of irrigated agriculture is expected. According to the Food and Agricultural Organization (FAO) a global expansion of irrigated agriculture with 30% by 2030 can be expected (Bof et al., 2013). Similar to the land use the first scenario is the analysis of the change between 1984 and 2013. Furthermore five future scenario's are analyzed in this research. For the future scenario's the irrigated area of 2013 is increased with 10, 20, 30, 50 and 100%.

4 | Method

Literature study, data analysis and hydrological modeling were the most important methods used within this research. Furthermore field visits were part of this study. Below the different parts of the research are further described.

4.1 Field visits

During the research the study area is visited two times. The main aim of these field visits was to get a realistic view of the study site. The report of the field visits can be found in Appendix A.

4.2 Hydrological Modeling

4.2.1 Model choice

An important part of this research was hydrological modeling. There are many hydrological models available for different purposes, all having their advantages and disadvantages. The criteria the model should fulfill for this research are:

- The model should be suitable for the analysis of climate and land use change.
- Because there will be many scenario's, which has to be calculated, the computational time of the model should be relatively low.
- The model should be able to simulate on catchment scale for large catchments, as the whole Paracatu Basin will be analyzed.
- The model should have a module to implement irrigation.
- The model should be open source and if possible be combinable with GIS.

Terink et al. (2015) give an short overview of the advantages and disadvantages of several hydrological models. According to this overview three models fulfill all criteria: SPHY, HYPE and SWAT. SWAT is chosen out of these three models, because it is already widely tested in different regions of Brazil and has great potential, according to Garbossa et al. (2011). Most of the papers reviewed in Garbossa et al. (2011) showed an adequate performance of SWAT and more than one third of these papers even present a monthly NSE (Nash-Sutcliffe Efficiency) of above 0.7.

4.2.2 Soil Water Assessment Tool - SWAT

SWAT (Soil Water Assessment Tool) is a physically based, hydrological model, developed by Dr. Jeff Arnold

for the USDA Agricultural Research Service (ARS) (Neitsch et al., 2011). It can be used for different scales, as watershed or river basin scale. Furthermore different hydrological processes can be simulated within SWAT, as well as the impact of climate- and land use changes and different land management strategies. Within this research ArcSWAT is used, a graphical user interface of the SWAT model within ArcGIS.

The major model components of SWAT are climate, hydrology, soil properties and land use. Data of all components is needed as model input and has to be edited before it can be used within the model. How the data is prepared is described in paragraph 4.3. Below the major steps of the model building are described.

Model building

The first step while building the model was determining the watershed. The watershed was determined based on the digital elevation map. Furthermore a mask with the boundary of the Paracatu River Basin was uploaded into the model. This mask was used to determine the boundaries of the project area. The next step was the stream definition. There is a choice between DEM-based stream definition and pre-defined stream definition. For the pre-defined stream definition two maps are needed, one with the subbasins and one with the main streams of the area. Both maps need special IDs to connect those maps to each other and to determine the flow direction of the streams. When using the pre-defined stream definition, the locations of the discharge stations (used for calibration) cannot be uploaded to the SWAT model. Therefore it is chosen to use the DEM-based stream definition. When choosing this method, SWAT determines the streams based on the digital elevation map. After the definition of the streams, the locations of the discharge stations can be uploaded. The next step was the watershed definition. First the outlet for the whole watershed was chosen. Based on the outlet and the digital elevation map, the river catchment and its subbasins were determined. Furthermore SWAT created an additional subbasin for each discharge station. The last step was the calculation of the subbasin parameters. The subbasin parameters were calculated by functions for calculating geomorphic characteristics of the subbasins and reaches (Winchell et al., 2013).

After the watershed delineation the HRU (Hydrological Response Units) were determined. HRUs are sub areas within a subbasin with homogeneous land use, soil

and slope properties. To determine these areas, the land use and soil map were uploaded into the model and were connected to the SWAT database by connecting the grid codes of the maps to the soil and land use types within this database. This can be done manually or by using look-up tables. For the slope, the amount of slope classes can be chosen and the borders of the different classes. In this research it was chosen to use 4 slope classes. The borders were determined based on the DEM using the "Slope"-tool of ArcGIS. This tool identifies the slope from each cell of a raster surface. After filling in the slope classes the HRUs were determined.

The last step in building the model was adding the climate data to SWAT. There is the choice between different methods to calculate evapotranspiration within SWAT: Priestley-Taylor, Penman-Monteith and Hargreaves (Neitsch et al., 2011). Dependent on the chosen method different amounts of climate input is necessary. Precipitation, minimum and maximum temperature and solar radiation is necessary for all three methods. In addition to this relative humidity is necessary for Priestley-Taylor and Penman-Monteith. For the Penman-Monteith method also wind data is needed. It was chosen to use Penman-Monteith, because it is recommended by FAO (Melo and Fernandes, 2012). In other researches one of the other methods might be chosen, because they need less input.

Calibration

The number of parameters, SWAT needs as input, is large, which makes the model parametrization and calibration more complicated. There are different approaches to calibrate a SWAT model, like manual calibration methods, automated methods and SWAT-CUP which combines automated and manually calibration in one decision tool (Arnold et al., 2012b). According to Arnold et al. (2012b) there are several steps to follow to calibrate the model well. The first step is a sensitivity analysis of the parameters. There are two types of analysis: local and global. When using the first method one parameter at a time is changed, while all parameters are allowed to change at the same time, when using the second method. After determining the most sensitive parameters, the calibration process can start. To calibrate the model, the model results (in this case discharge) are compared with the observed data. When the difference is too large, parameters have to be changed again until the results of the model are close enough to the measured values. To test if the model is also working for other time periods, a validation has to be carried out. Therefore the model will be used to simulate another period than the calibration period,

while using the same parameters.

There are different ways to test if a model can be called satisfactory. In many researches the Nash-Sutcliffe efficiency (NSE) is mentioned as one criteria to test the model performance (Arnold et al., 2012b; dos R. Pereira et al., 2016; Moriasi et al., 2007). Other types of criteria, which also can be found in the papers just mentioned are the percent bias (PBIAS) and the the RMSE-observations standard deviation ratio (RSR). RMSE stands for root mean square error. According to Moriasi et al. (2007) a model can be called satisfactory if the $NSE > 0.5$, the $RSR \leq 0.7$ and the $PBIAS \pm 25\%$. The values for NSE, RSR and PBIAS can be calculated with the equations below.

$$NSE = 1 - \left[\frac{\sum_{i=1}^n (Y_i^{obs} - Y_i^{sim})^2}{\sum_{i=1}^n (Y_i^{obs} - Y^{mean})^2} \right] \quad (1)$$

$$PBIAS = \left[\frac{\sum_{i=1}^n (Y_i^{obs} - Y_i^{sim}) * 100}{\sum_{i=1}^n (Y_i^{obs})} \right] \quad (2)$$

$$RSR = \frac{\sqrt{\sum_{i=1}^n (Y_i^{obs} - Y_i^{sim})^2}}{\sqrt{\sum_{i=1}^n (Y_i^{obs} - Y^{mean})^2}} \quad (3)$$

where Y_i^{obs} is the observed discharge on day i , Y_i^{sim} the simulated discharge by the model and Y^{mean} the average discharge of the observed values.

Within this research the model was calibrated manually, by using the "manual calibration helper" (Winchell et al., 2010) and the "SWAT Check" (White et al., 2014). As calibration years 1984 and 1985 were chosen and as validation years 1986 and 1987, because for these years discharge data was available without gaps. Furthermore during this period there was nearly no irrigation, thus are representative for a "natural" situation. The model was calibrated for the Porto Alegre station, because it is the most downstream discharge measurement station before the outlet of the Paracatu Basin.

First all parameters inside the manual calibration were analyzed, based on their relevance for the research. Parameters regarding snow, water quality etc. are not relevant for this research and were therefore left out in the calibration process. The remaining parameters and their definitions can be found in table 4.1. Ranges of parameters in the table indicates that the parameters are different for different subbasins. The second step of the calibration process was a sensitivity analysis. Therefore the model was tested several times, with changing one parameter with every test. After changing each

Table 4.1: Calibration parameters and their values before and after calibration, source of the definitions: Arnold et al. (2012a)

Parameter	Definition	Unit	MIN	MAX	before calibration	after calibration
SURLAG	Surface runoff lag time	days	1	24	4	4
ALPHA_BF	Baseflow alpha factor for deep aquifer	1/days	0	1	0.048	0.55
GW_DELAY	Groundwater delay	days	0	500	31	150
GW_REVAP	Groundwater "revap" coefficient	-	0.02	0.2	0.02	0.02
GWQMN	Threshold depth of water in the shallow aquifer required for return flow to occur	mm	0	5000	1000	700
RCHRG_DP	Deep aquifer percolation fraction	-	0	1	0.05	0.1
REVAPMN	Threshold dept of water in the shallow aquifer for "revap" to occur	mm	0	1000	750	750
CANMIX	Maximum canopy storage	mm	0	100	0	0
EPCO	Plant uptake compensation factor	-	0.01	1	1	1
ESCO	Soil evaporation compensation factor	-	0.01	1	0.95	0.01
SLOPE	Average slope steepness	m/m	0	0.6	0.006-0.43	0.003-0.21
SLSUBBSN	Average slope length	m	10	150	9-121	9-121
CN2	SCS runoff curve number for moisture condition 2	-	35	98	60-92	45-69
CH_K2	Effective hydraulic conductivity in main channel alluvium	mm/h	0	500	0	0
CH_N2	Manning's "n" value for the main channel	-	0.01	0.3	0.014	0.09
SOL_ALB	Moist soil albedo	-	0	0.25	0.08	0.08
SOL_AWC	Available water capacity of the soil layer	mm/mm	0	1	0.13-0.21	0.13-0.21
SOL_K	Saturated hydraulic conductivity	mm/h	0	2000	100-1686	50-843
SOL_Z	Surface runoff lag time	mm	0	3500	800-3460	800-3460

parameter once, it was analyzed which parameters had the biggest impact on the results. The most sensitive parameters within this research were GW_DELAY, GWQMN, RECHARGE_DP and SLOPE. Actually also other parameters were changed during the calibration process, because sometimes a parameter was more sensitive if combined with a different specific value of another parameter.

The third step was the calibration process itself. The calibration process consisted of several steps, which had been repeated several times, until the result became satisfactory. One calibration cycle started with changing one parameter. After the model test, the results were analyzed inside the SWAT check (see figure 4.1), to see which flows were too high or too low. Afterwards the simulated discharge per day was compared to the measured values. By using the SWAT check in addition to the comparison with the measured values, more insight in the working of the model was given. Furthermore the NSE was calculated after each test. If the NSE became higher after the test, the new parameter value was adapted, if the result became worse, the parameter

was set to the value it had before.

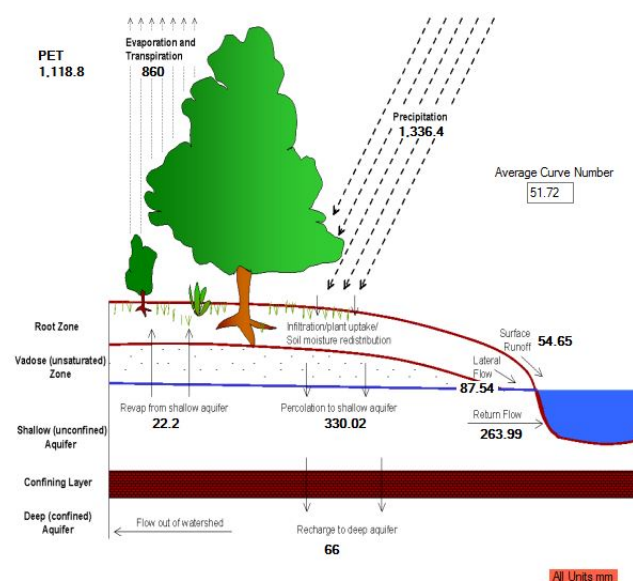


Figure 4.1: Example of the SWAT check inside ArcSWAT, developed by White et al. (2014)

In figure 4.2 three graphs can be seen. The first graph shows the simulated discharge (blue) before calibration compared with the observed discharge (green). The NSE of this model test is negative (-4.75). The second graph shows the results after the calibration. The NSE is above 0.6 (0.66), the PBIAS has a value of -26.19 and the RSR has a value of 0.58. Thus the model fulfill two of the three criteria described in Moriasi et al. (2007) and is judged to be satisfactory. The value for the NSE of the validation (graph 3) is slightly lower and the PBIAS and RSR value slightly higher, but also here two of the three criteria are fulfilled. To get the model calibrated nine parameters were changed. The initial values (before calibration) of each parameter were determined by SWAT automatically, based on default values and input tables (e.g. soil characteristics). The initial values and the final values (after calibration) per parameter can be found in table 4.1. The parameters indicated in grey are the one which were changed.

In the first tests the model reacted very quickly to rain events and the flow becomes zero often, when there was no rain. Therefore the reaction time of the water system inside the model had to be slowed down. This is done by changing the GW_DELAY from 31 to 150, to simulate a longer period for the ground water flow reaching the river and a larger groundwater storage. Furthermore the total amount of discharge was very large during the first tests without calibration. One reason for this high amount of water inside the reach was a low evapotranspiration. By decreasing the ESCO (Soil evaporation compensation factor) more water can be extracted for the ET demand. This resulted in lower peaks and a lower total amount of available water in the reaches. The CH_N stands for the river roughness. The initial value of the CH_N was very small, which stands for a very low river roughness of reaches without vegetation and obstacles inside the river to slow down the water. This value was increased to a more realistic value to simulate a river with more vegetation. The SOL_K (saturated hydraulic conductivity) was decreased. This resulted in smaller peaks and a slower response to rainfall events, because water needs more time to flow through the soil due to the lower conductivity.

After the first calibration steps the peaks were still high, due to a high surface flow. To reduce the surface flow, the CN2 (SCS runoff curve number) was decreased. At the same time the return flow needed to be increased to get more baseflow. The return flow and thereby the base flow was increased by changing the GWQMN. GWQMN stands for the threshold depth of water in the shallow aquifer required for return flow to occur. By decreasing the GWQMN from 1000 to 700mm,

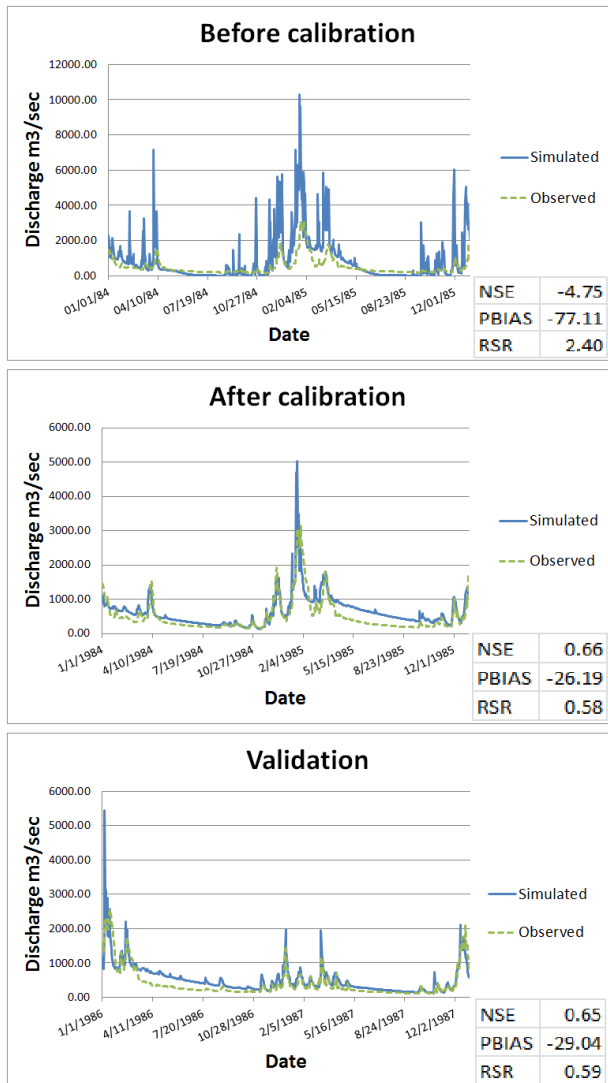


Figure 4.2: Baserun, calibration run and validation run compared to the observed values

the return flow became higher, which resulted in an increase in baseflow. Actually after this modification the simulated baseflow was higher than the observed baseflow for some periods. Therefore the ALPHA_BF (baseflow alpha factor for deep aquifer) was increased. A factor between 0.1 and 0.3 stands for an area with a slow response and a factor between 0.9 and 1.0 for an area with fast response. The initial value was very low, which resulted in a slow response of the area. By increasing the factor to 0.5 the response time decreased which resulted in a small decrease of the baseflow.

After changing 7 parameters the simulated total amount of water available in the reach was still higher than the observed amount of water. To decrease the total amount of water, the flow to the deep aquifer had to be increased. This was done by increasing the RCHRG_DP

(deep aquifer percolation fraction). Also the lateral flow was still very high after the first parameter changes. To reduce the lateral flow the average slope steepness (SLOPE) was decreased. This had led to a decrease in lateral flow and lower peaks.

4.3 Data analysis and editing

The main part of the research consisted of literature study and data analysis. Literature and data was collected as input for the model and for the scenario analysis.

For this research several data sources were used. A large part of the data is provided by or via Embrapa. Another part of the data is based on global data sets, scientific literature and other data sources. Below the used data is described in more detail, including the most important editing steps to get SWAT input and the data source. In addition to this an overview can be found in Appendix C of all data with its sources and all editing steps.

4.3.1 General data

Digital Elevation Map

Digital Elevation Maps (DEM) are available from different sources. Three DEMs of different sources were analyzed for this research to find the most suitable DEM for the model. The three sources were NASA, Hydroshed and INPE.

The SRTM grid from NASA is available with a 3 arc-second (ca. 90m) and a 1 arc-second (ca. 30m) resolution. Hydroshed offers a hydrological conditioned DEM, based on the SRTM grid of NASA with a resolution of 3 arc-seconds. The digital elevation map of INPE has a resolution of 1 arc-second. Furthermore INPE offers additional data to the grid, e.g. slope. The Hydroshed-DEM has a big advantage, because it is hydrological conditioned and therefore very suitable for modelling studies. But even though it has this advantage it was not chosen for this research, because the resolution of the INPE-DEM and the SRTM grid are higher. For this research a high resolution is of importance for SWAT to determine the subbasins and hydrological response units well, based on the elevation. The INPE-DEM is chosen instead of the SRTM grid, because it has a lot of additional data available to adjust the input where necessary.

Boundaries

EMBRAPA provided two shape-files from the IBGE

(Brazilian Institute of Geography and Statistics) with boundaries. One shape-file contains the boundary of Brazil and the other one the boundaries of the different Brazilian states. These shape-files are used for creating the location map of the study area and are not used within the SWAT model. Therefore these files are not further edited.

4.3.2 Hydrological data

All hydrological data is provided by EMBRAPA and comes originally from ANA (National Agency of Water, Brazil).

Rivers and Streams

The first part of the hydrological dataset are different shape files of the rivers and streams in the area. There is one shape file with the location of the São-Francisco River, one with the location of the Paracatu River and one of the Preto River. These shape files are only used to make a map indicating the location of the rivers and therefore they are not further edited.

Furthermore a shape file is provided with all small streams and tributaries of the Paracatu River. Based on this stream file and the report of Rodriguez (2004), the most important streams of the Paracatu River are determined. This shape file of the main streams is used to imprint the rivers into the SWAT model at places, where the DEM is not sufficient enough to determine the smaller rivers. It is not used as input for the pre-defined rivers, because the watersheds inside this model are DEM-based and not pre-defined.

Basins and sub-basins

Shape files are provided with the boundaries of the Paracatu River Basin and the Preto River Basin. The file of the Preto River Basin is as the River shape files only used to indicate the location in maps. The Paracatu River Basin file is furthermore used for creating a mask file as input for the SWAT model, by transforming it into a raster. The subbasin file is edited by splitting some subbasins, based on the digital elevation map and the location of the streams, in order to have one subbasin per main stream. These pre-defined subbasins are not equally to the subbasins generated by the SWAT model.

Discharge data

The discharge data consists of measurements of 33 stream gauge stations in- and outside the Paracatu River Basin, which can be used for the model calibration. First it was analyzed of which stations and which years the data is most complete. For the calibration the

Porto Alegre station is chosen, because it is the most downstream station before the outflow point of the basin. As calibration years 1984 and 1985 are chosen, because in this period there was nearly no irrigation and therefore a natural situation can be assumed. Furthermore these years, as well as the validation years (1986 and 1987) have no missing values for this station.

For the irrigation scenario's the years 2010 and 2011 are used. The discharge time series of 2011 has missing values for 34 days. The time series is gapfilled, using the Cachoeira do Paredao discharge station, which is located upstream of the Porto Alegre station. The gapfilling is done with the following equation:

$$D_1 = \frac{A_1}{A_2} * D_2, \quad (4)$$

where

D_1 is the discharge, which has to be calculated,

A_1 is the drainage area belonging to the station with missing values,

A_2 is the drainage area belonging to the station, used for gapfilling,

D_2 is the discharge of the station, used for gapfilling.

4.3.3 Meteorological data

The Meteorological data consist of rainfall stations and meteorological stations with different weather parameters. The location of the different stations can be found in appendix B

Rainfall stations

The rainfall data set consists of measurement at 103 stations and is provided by ANA. First the rainfall stations with the most complete and longest time series are chosen. The criteria are that the time series need to start before or in 1984 and do not end earlier than 2006 to have a long enough time series. The second criteria is that the maximum of missing values must be below 10% of the total amount of values. By applying these criteria, the number of rainfall stations was decreased to 37.

Within the SWAT model, there is a weather generator to gapfill meteorological data based on statistical values of the different parameters (see chapter 12 of Arnold et al. (2012a)). Because the weather generator of SWAT needs a large amount of input to generate missing rainfall data, there is chosen to gapfill the rainfall data manually in advance. To have some warm up years and years to base the climate scenario's on, the rainfall data is gapfilled for the period from 1975 to 2005. This is

done per station with data from close-by rainfall stations.

Meteorological stations

There are two types of meteorological data provided by EMBRAPA. The first type of meteorological data consists of monthly average temperature and rainfall only and is originated from INMET (National Institute of Meteorology), INPE (National Institute of Space Research), EMBRAPA, ANA (National Water Agency), CEMIG (Minas Gerais Energy Company) and CPRM (Geological Survey of Brazil). The second data type consists of more parameters, like maximum and minimum temperature, sun hours, wind speed and relative humidity. This data is delivered by INMET only. For this research only the second data type is used, because it is more complete and these data are required for the Penman-Monteith equation to calculate evapotranspiration.

The first step in editing the meteorological data is to convert the sunshine hours to solar radiation in MJ/day. Therefore the formulas of Angstrom Allen et al. (1998) are used:

$$R_s = (a_s + b_s \frac{n}{N}) R_a \quad (5)$$

In which

- R_s is solar or shortwave radiation [$\text{MJ m}^{-2}\text{day}^{-1}$],
- n is the actual duration of sunshine [hour],
- N is the maximum possible duration of sunshine or daylight hours [hour]
- R_a is the extraterrestrial radiation [$\text{MJ m}^{-2}\text{day}^{-1}$],
- a_s is the regression constant, expressing the fraction of extraterrestrial radiation reaching the earth in overcast days ($n=0$),
- $a_s + b_s$ is the fraction of extraterrestrial radiation reaching the earth on clear days ($n=N$).

For a_s and b_s the values 0.25 respectively 0.5 are used, like recommended in Allen et al. (1998), when no calibration can be carried out to improve these parameters. n is measured at the meteorological stations.

N is calculated by:

$$N = \frac{24}{\pi} \omega_s \quad (6)$$

where ω_s is the sunset hour angle in radians, which is calculated by

$$\omega_s = \arccos[-\tan(\varphi)\tan(\delta)] \quad (7)$$

φ is the latitude in radians and δ is the solar declination in radians calculated as follows:

$$\delta = 0.409 \sin\left(\frac{2\pi}{365} J - 1.39\right) \quad (8)$$

where J is the number of the day of the year between 1 (1st January) and 365 or 366 (31st December).

R_a is calculated with the following formula:

$$R_a = \frac{24(60)}{\pi} G_{sc} d_r [\omega_s \sin(\varphi) \sin(\delta) + \cos(\varphi) \cos(\delta) \sin(\omega_s)] \quad (9)$$

In which

- R_a is the extraterrestrial radiation [$\text{MJ m}^{-2}\text{day}^{-1}$],
- G_{sc} is the solar constant = $0.0820 \text{ MJ m}^{-2}\text{day}^{-1}$,
- d_r is the inverse relative distance Earth-Sun,
- ω_s is the sunset hour angle [rad] (see equation 3),
- φ is the latitude [rad],
- δ is the solar declination [rad] (see equation 4).

d_r is calculated by:

$$d_r = 1 + 0.033 \cos\left(\frac{2\pi}{365} J\right) \quad (10)$$

where J is the number of the day in the year.

After transforming the sun hours into solar radiation, all meteorological data is gapfilled. For the years 1980 to 2005 the data is gapfilled with data from Xavier et al. (2016). For the period from 1975 to 1980 the timeseries are gapfilled by the average of close-by meteorological stations, due to a lack of alternative data sources. Another source for radiation data could be the radiation data provided by NASA (NASA, 2016). The data is compared to the transformed sun hours from INMET (see figure 4.3). With an R^2 value of 0.8 the data provided by NASA would be suitable for the research. Actually it is not chosen to use this data, because for this area enough measured data has been available. But the NASA data can be used for other areas close-by where no measured data is available or for years without measured data.

4.3.4 Land use and soil data

Another important input for the SWAT model is land use and soil data. Below the editing steps of these two maps are described.

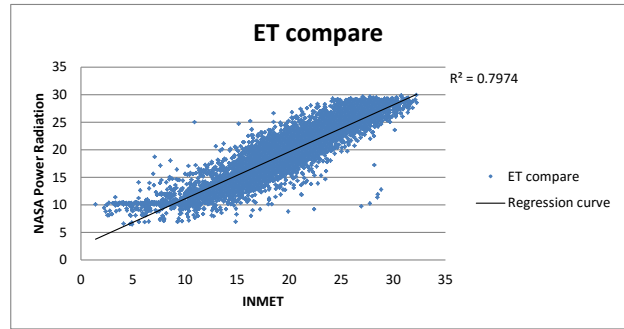


Figure 4.3: Radiation data provided by NASA compared to transformed radiation based on sunshine hours

Land use data

There are two shape files provided by EMBRAPA with the land use of the years 1984 and 2013. These maps are made, based on Landsat TM5 images. The water areas are missing on the 1984 land use map. It is assumed that the water areas haven't changed much during the last 30 years, so the water areas of 2013 are added to the 1984 land use map. Furthermore the names of some classes differ between the two land use maps. Also some classes are divided into subclasses. To make comparison between the two maps more easy, these subclasses are merged into one class and the names are changed, so that both land use maps have the same amount of classes and the same names for each class. In the map of 2013 no difference is made between irrigated and rain-fed agriculture. To implement irrigated areas into the 2013 land use map, the locations of the center-pivots are added to the land use map. To use both maps as SWAT input, they are transformed into grid files with one grid value per land use class. Afterwards a look up table for each grid is created to couple these grid codes to land use types within the SWAT database. Soybean is used as representative crop for rain-fed agriculture within SWAT and corn as representative crop for irrigated agriculture.

Soil data

For the soil map two soil maps of the IBGE database (IBGE, 2016) are combined. The values of the different soil parameters (hydraulic conductivity etc.) are based on Mingoti et al. (2015). After combining the two maps, the soil map is transformed into a grid with one grid value for each soil type. The parameters are filled into the SWAT database and connected to the soil map.

4.3.5 Climate and land use change data

To implement climate and land use change into the SWAT-model, new input data has to be created.

Below the method for the different scenario's is explained.

Climate change

The dataset available for climate change is provided by INPE (2016). The dataset consist of results for different climate parameters (precipitation, temperature etc.) of the two climate models HadGEM2-ES and the MIROC-5 model (described in chapter 3). There are four different time series, per model, pathway and parameter: a historical time series going from 1961 to 2005 and three future time series going from 2007 to 2040, 2041 to 2070 and 2071 to 2099. Because there can be some uncertainties in the results of the climate models, it is chosen to edit the data, using two different methods, here called BIAS-correction method and the Delta method. According to Teutschbein and Seibert (2012) the delta-change approach (here called Delta method) is "a stable and robust method that produces future time series with dynamics similar to current conditions. Both methods will be described below, after describing the general editing steps needed for both methods.

General editing steps

The methods are applied for the following meteorological parameters: precipitation, maximum and minimum temperature, solar radiation, relative humidity and wind speed. First step is to calculate the monthly average of all time series per station, including the measured values of the different parameters. After calculating the averages of all stations, the values are interpolated between the stations. To make them more comparable to the measurement stations, the interpolated values are extracted to the locations of the measurement stations.

BIAS-correction method

The assumption behind the BIAS correction method is, that the climate models over- or underestimate the reality. Therefore the historical time series of the model are compared with the measured values. Based on this the bias can be calculated and used to correct the future time series of the models. For all parameters the bias is calculated with the following formula:

$$B = \frac{(meas - mod_{historical})}{mod} * 100 ,$$

where B stands for the bias, "meas" for the measured monthly average and "mod" for the modeled historical monthly average.

With the calculated bias all daily values of the time series of the climate models are corrected:

$$x_{cor} = x_{ori} * (1 + \frac{B}{100}) ,$$

where x_{cor} stands for the corrected daily value, x_{ori} for the original daily value and B for the calculated bias.

Delta method

The delta method assumes that the climate models predict the climate changes in future well. But the future time series are based on the historical time series of the models. To get future time series based on real measured values, the delta (change between historical and future situation) has to be calculated for all future time series and then be applied to the measured time series. The delta for precipitation, solar radiation, wind speed and relative humidity is calculated per month as follows:

$$\Delta = \frac{mod_{future}}{mod_{historical}} ,$$

where Δ is the delta, mod_{future} the modeled monthly average of the future time series and $mod_{historical}$ the modeled monthly average of the historical time series.

For temperature the delta is calculated with a different formula:

$$\Delta = mod_{future} - mod_{historical} .$$

With the calculated deltas new future time series are created, based on the time series with measured values. Therefore measured historical time series are chosen, with the same length like the future time series:

- 1975-2005 for future time series 2010-2040
- 1976-2005 for future time series 2041-2070
- 1977-2005 for future time series 2071-2099

The chosen historical time series for precipitation, solar radiation, wind speed and relative humidity are changed using the following equation:

$$x_{future} = x_{historical} * \Delta$$

Because the delta for temperature is calculated differently, also the values for the time series are calculated slightly different:

$$x_{future} = x_{historical} + \Delta$$

In both equations x_{future} is a daily value of the future time series, $x_{historical}$ a daily value of the historical, measured time series and Δ the delta of the month, the

daily value belongs to.

Land use change

To analyze the historical land use change scenario, the land use map of 2013 is uploaded into the SWAT model and is calculated using the same climate data as for the model with the land use map of 1984. Using the same climate data, this factor is assumed to be constant and all changes in results can be assumed to be based on the change in land use. For the future scenario's the land use is updated within the SWAT model. This is done by using the Land use update option within ArcSWAT. This method allows a change of one land use type at a time into other land use types. The changes are filled in into the model as percentages. Because it is not possible to change two land use types at a time, the last Future scenario is simulated by using a new created land use map.

The first step to create this land use map is to create a random raster, with values from 0 to 100. These numbers can later be used as percentages, when defining the new land use classes. For this case agriculture should increase with a decrease in pasture of 30% and a decrease in savanna of 20%. First the change in pasture will be calculated. Therefore the random raster is used. All cells of the random raster with a value between 1 and 70 will get the grid number of pasture and all other cells will get the grid number of rain-fed agriculture. This result in a grid with random located cells, whereby 70% is pasture and 30% is rain-fed agriculture. The next step is to update the land use map of 2013 with the edited random raster. This is done by replacing the cells of pasture in the land use map of 2013 with a cell of the random raster. This results in a new land use maps. Afterwards the cells of the first random raster are replaced by 80% savanna and 20% agriculture. Then the new land use map is updated by replacing the cells with the grid number of savanna with cells of the new random raster. The resulting land use map is used in the SWAT model to simulate the 5th future scenario.

Irrigation scenario's

As there was no detailed irrigation data available for this research, the decrease of discharge due to irrigation had to be determined differently. To determine the decrease in discharge due to irrigation, the observed discharge for the years without irrigation (1984 and 1985) were compared with the observed discharge values of the years with irrigation (2010 and 2011). It is assumed that the decrease in discharge is caused by irrigation only. But other factors like changing rainfall can also be cause of the decrease in discharge. Therefore the influence of precipitation on the changing discharge was analyzed

first. To determine the influence of rainfall during the dry period, when irrigation is applied most, the monthly averages of the discharge for both periods were divided by the monthly averages of the rainfall. This ratio was multiplied by 100. In figure 4.4 the ratios for the two periods are shown. If the distance between the two lines is very low, it means that the ratio is nearly the same of both periods and therefore the precipitation has been of large influence. For the dry period the difference between the two ratios is large. This means that rainfall is of less influence during this period.

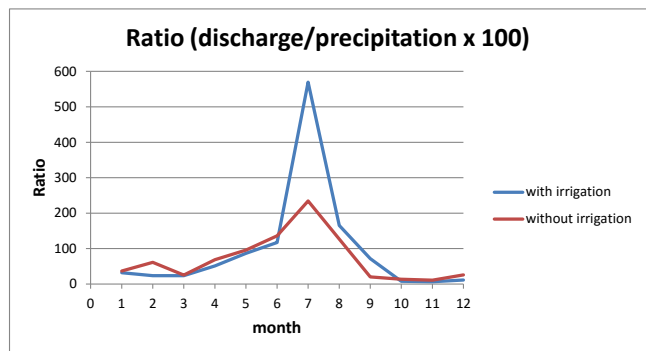


Figure 4.4: Ratio of discharge and precipitation, based on monthly averages

After determining the ratio, the analysis of the decrease in discharge due to irrigation was continued. The decrease in discharge due to irrigation is calculated by determining the monthly average discharges for both period and subtracting these values from each other (see figure 4.5). The result is a decrease of discharge in m³/sec. The next step was to determination of the increase in irrigated areas between the two periods. Therefore the land use maps of 2013 and 1984 are compared. Based on the difference in irrigation area and the decrease in discharge, the decrease in discharge per one square-meter increase of irrigated area was calculated. This was done by dividing the average decrease in discharge per month by the amount of areal increase. Hereby a linear relationship between the increase in irrigation areas and the decrease in discharge is assumed.

To analyze how further increase in irrigated agriculture will influence the discharge in future, the irrigated area of 2013 was increased by another 10, 20, 30, 50 and 100%. Then the increase in irrigated areas was calculated in square-meter by subtracting the original area (from 1984) from the new irrigated area. This difference was multiplied with the ratio of decrease in discharge per square-meter increase of irrigated areas. This resulted in absolute decreases in discharge per month for the different

irrigation scenario's. To calculate the monthly average discharge values for the different irrigation scenario's, the decrease in discharge was subtracted from the monthly average discharge values of 1984/1985.

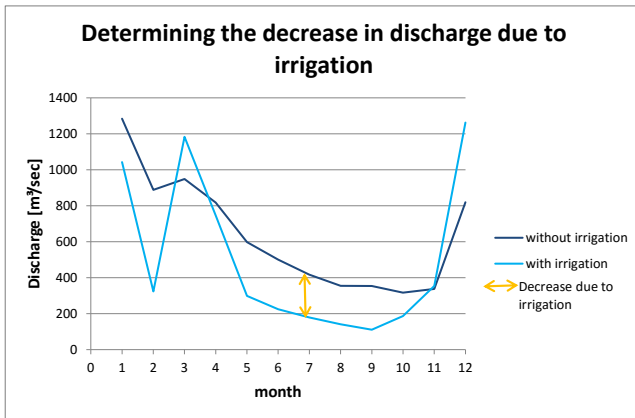


Figure 4.5: Determination of decrease in discharge due to irrigation

5 | Results

The model is run several times to get discharge results for different scenario's. Below the results of the current situation, as well as the climate, landuse and irrigation scenario's are described and analyzed.

5.1 Current discharge characteristics

In figure 5.1 the monthly averages of the simulated (blue line) and observed discharge (red line) at the Porto Alegre Station are shown. For both, the simulated and the observed discharge, the values are highest during January, which is in the rainy period of the year. The lowest discharge values can be found during the dry period with the lowest observed discharge values in August. The wettest months December, January and February are well simulated by the model. But as it gets dryer the model overestimates the discharge.

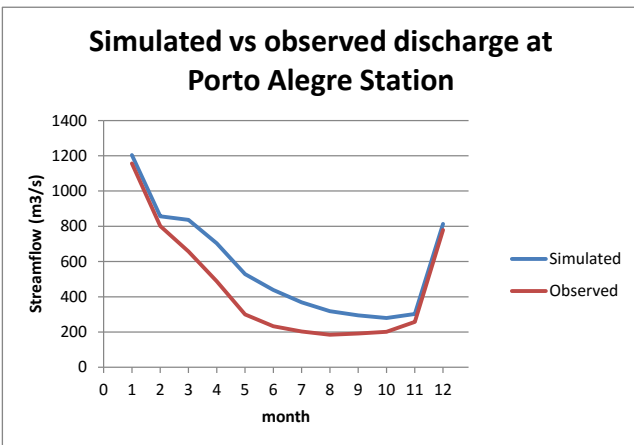


Figure 5.1: Monthly averages (1984-1986) of observed and simulated discharge at Porto Alegre station

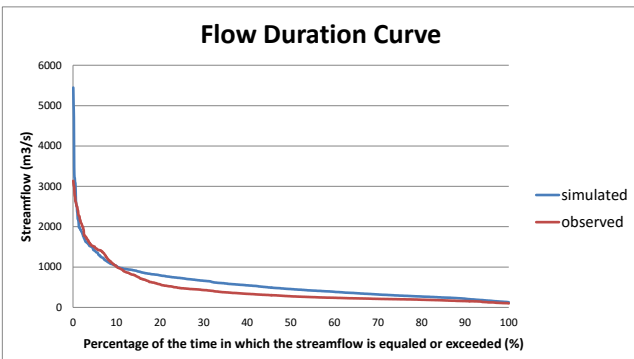


Figure 5.2: Flow duration curve, Porto Alegre, 1984-1986

That the model overestimates the discharge values compared to the observed values, can also be seen in figure 5.2. In figure 5.2 the flow duration curves of the

observed and the simulated discharge values are shown. The highest discharge of the simulated values lies between 5000 and 6000 m³/sec, while the highest observed value lies around 3000 m³/sec. This means that the model simulates some extremer peaks. Less extreme discharges which are equaled or exceeded 1-10% of the time, are nearly the same for both cases. Lower discharges (with an 10-80% occurrence) are overestimated by the model.

5.2 Impact of climate change on water resources

As explained in chapter 4 and chapter 3 two climate models with two representative concentration pathways each are used to analyze climate change. To correct the climate time series of the climate models the BIAS-correction and the Delta-method are used. This results in eight sets of climate data (four sets of each climate model), which can be found in appendix D.

5.2.1 ETA HadGEM2-ES

In figure 5.3 the results of the four ETA HadGEM2-ES datasets are shown. Per dataset three periods are calculated: 2007-2040 (green line), 2041-2070 (orange line) and 2071-2099 (red line). These periods are compared to the results based on measured climate data (1975-2005, blue line).

In all cases there is a big decrease in discharge. For the rcp 4.5 scenario (BIAS-corrected) the biggest decrease in discharge takes place between 2007 and 2040 with an average decrease of 450m³/sec. The decrease for the period between 2041 and 2070 is lower (329m³/sec). The smaller decrease in the second period compared to the current situation is caused by a smaller decrease in rainfall during that period. While the average decrease in precipitation is 37mm/month between 2007 and 2040, the average decrease for the second period (2041-2070) is 24mm/month. This is caused by more extreme weather events. The maximum rainfall between 2007 and 2040 is 90mm/day, while the maximum rainfall between 2041 and 2070 is 133mm/day. The rainfall events of the third period (2071-2099) are also more extreme with a maximum of 130mm/day, but the total amount of rainfall is less than in the second period. This results in an average decrease in discharge of 346m³/sec.

In all periods the biggest absolute decrease of discharge takes place in March with resp. 744, 563 and

613m³/sec. The biggest relative decrease takes place between June and August with 78% for the first period and in December for the second period with 62%. The biggest relative decrease of the third period takes place in March with 62%. This is not fully consistent with the decrease in rainfall. For rainfall the biggest absolute decrease takes place in November and December with resp. 96 and 100mm/month, 92 and 86mm/month, 64 and 89mm/month. The biggest relative decrease takes place between June and July with decreases of resp. 78 and 83%, 74 and 71%, 69 and 56%. This means that rainfall is of large influence, but is not the only factor affecting the discharge.

Temperature increases in all cases, with the lowest increase in the first period and the highest increase in the third period. Solar radiation decreases for the first period. The other two periods have a decrease during the dry period and a slightly increase in the first months of the year. Furthermore there is a large increase in wind speed and a decrease in relative humidity. The changes of the other climate parameters also have influence on the decrease in discharge.

The decrease in discharge for rcp 8.5 is higher than the decrease in discharge for rcp 4.5. For the different periods the decrease in discharge is resp. 477m³/sec (80%), 494m³/sec (84%) and 511m³/sec (87%). The month with the largest absolute decrease is like in the first scenario March with decreases of resp. 811, 823 and 838m³/sec. The relative decrease in discharge is largest in January, July, August and December with 82% each for the first period. The largest relative decrease takes place in August with 88% for the second period and in November with 91% for the third period.

That the largest decrease in discharge can be found in the third period is consistent with the decrease in rainfall. While the rainfall decreases with 42% in the first period, the decrease of the third period is 54%. Like in the case before, November and December are the months with the largest absolute decrease for all periods. The relative decrease in rainfall takes place in resp. December (67%), November (68%) and November (83%). The change of the other climate parameters is similar to the rcp 4.5 scenario's.

For the scenario's in which the Delta-method is used, the decrease in discharge is higher than in the scenario's of the BIAS-correction method. The average decrease in discharge of rcp 4.5 for the different periods is resp. 491, 420 and 449 m³/sec. The pattern with the largest decrease in the first period is similar to the BIAS-corrected sce-

nario. For the rcp 8.5 the average decrease is resp. 526, 513 and 558 m³/sec. Therefore the pattern is slightly different to the BIAS-corrected method, where the second period has a higher average decrease than the first period. The months with the largest absolute decrease are different for the rcp 4.5 scenario of the Delta-method. In this case January is the month with the largest average decrease for all periods, while for the rcp8.5 scenario of the Delta-method it March is again the month with the largest decrease. The period between June and August are for all periods in both cases the time with the largest relative decreases. For the rcp4.5 case this is in consistent with the largest decrease in rainfall in the same period. For the rcp 8.5 scenario the largest decrease in rainfall takes place around November and December. The change of the other climate parameters is similar to the changes using the BIAS-correction method.

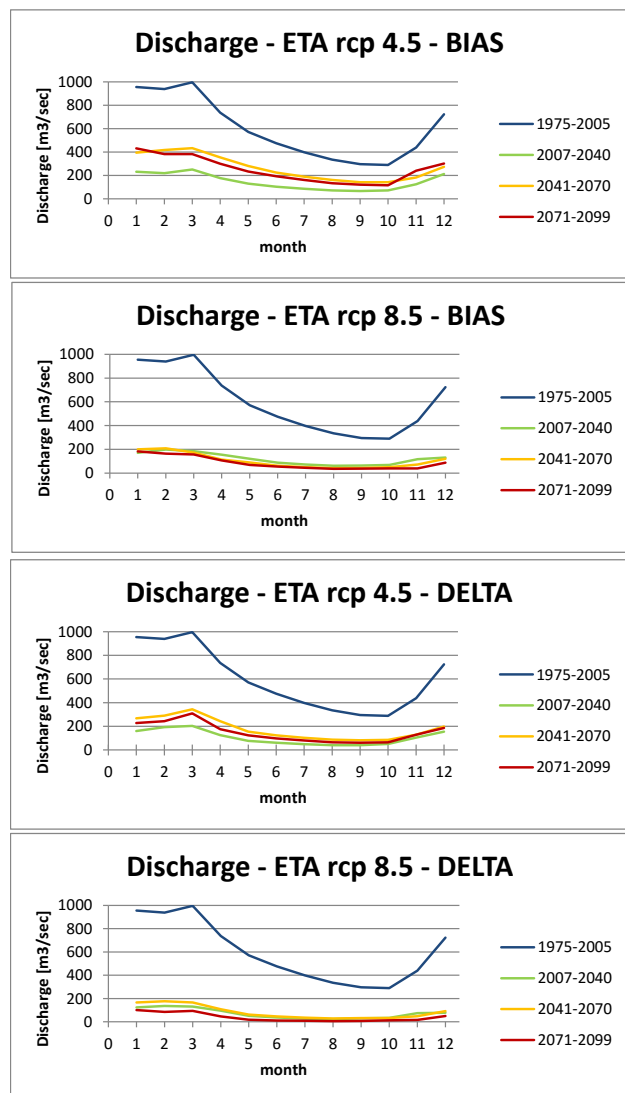


Figure 5.3: Monthly averages for different climate scenario's (ETA-model) at the Porto Alegre station

5.2.2 ETA MIROC 5

Figure 5.4 shows the model results using the ETA-MIROC5 climate data as input. In all cases there is a significant decrease in discharge. For the bias corrected rcp 4.5 scenario the average decrease in discharge is largest for the second period (2041-2070) with a decrease of 293 m³/sec (29%) and lowest for the first period with a decrease of 179m³/sec (49%). In all periods March is the month with the largest absolute decrease. The decrease in rainfall is consistent with the decrease in discharge. The largest average decrease in rainfall takes place in the second period and in all periods the absolute decrease in rainfall is largest in March. But different to the scenario's of the ETA HadGEM2-ES model, there are also several months with a significant increase of rainfall. The largest increase of rainfall takes place in resp. January (90mm/month), February (15mm/month) and January (74mm/month). The increase in rainfall leads to a lower average decrease in rainfall during the whole period and therefore a lower decrease in discharge, compared to the scenario's of the ETA HadGEM2-ES model. The change of the other climate parameters show a similar pattern to the changes using the ETA HadGEM2-ES model. The bias corrected rcp 8.5 dataset leads to slightly larger decreases in discharge (255, 276 and 293 m³/sec). Again March is the month with the largest absolute decrease. The absolute decrease in rainfall is also highest in March for the first and third period.

The input data sets corrected with the Delta-method lead to lower decreases in discharge in most of the scenario's. For the rcp4.5 the decreases are resp. 174, 250 and 255 m³/sec, with the largest absolute decrease in March for all periods. Again the decrease in rainfall follows a similar pattern, with highest decrease in March and an increase of rainfall during the begin of the year. For the rcp 8.5 scenario the decrease in discharge is highest for the third period with a decrease of 335 m³/sec. For all three periods the absolute decrease is largest in March with resp. 460, 435 and 600 m³/sec decrease. That the decrease in discharge is highest in the third period is consistent with the decrease in rainfall, which is also highest for the third period. The change of the other weather parameters are similar to the other scenario's.

5.2.3 Summary of the climate change results

In appendix E a summary of the climate change results can be found. For both climate models and both correction methods the rcp 8.5 leads to bigger decreases in

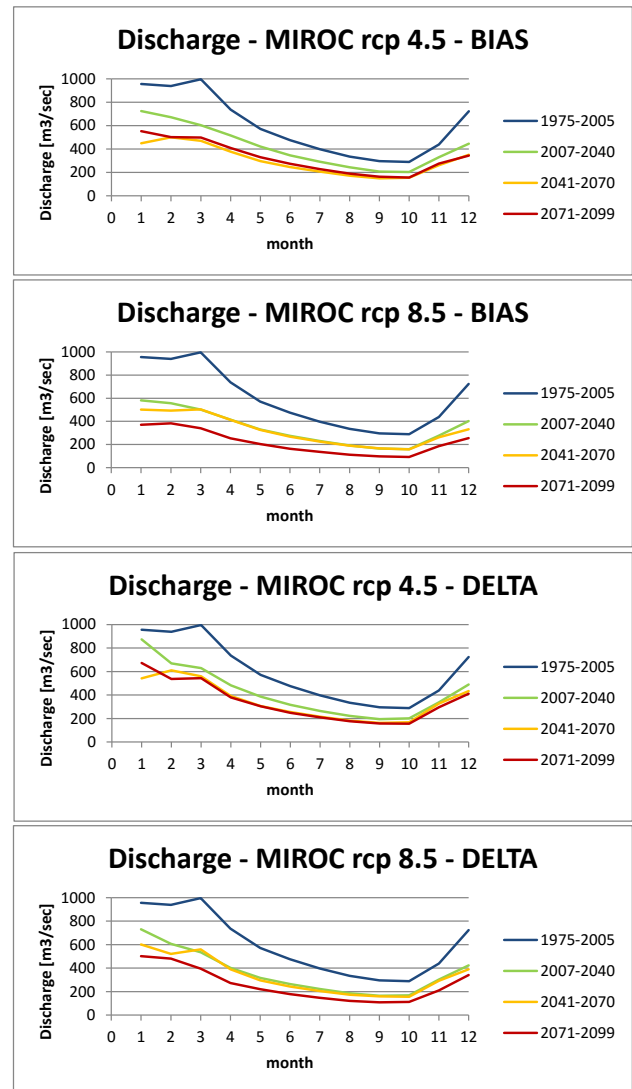


Figure 5.4: Monthly averages for different climate scenario's (MIROC-model) at the Porto Alegre station

discharges. Using the ETA HadGEM2-ES climate data as input results in larger decreases compared to the ETA MIROC5 model. While the Delta-method results in larger decreases compared to the BIAS-correction method when using the ETA-HadGEM2-ES model, it is the other way around when using the ETA-MIROC5 model. In nearly all cases March is the month with the biggest absolute decrease in rainfall. The main reason for the decrease in discharge is the decrease in rainfall, but also the other climate parameters are of influence on the water availability. By changing the weather parameters, the evapotranspiration changes and thereby the water availability changes also. Dependent on which model and correction methods are used the discharge is expected to decrease with an amount between 29 and 89% for the first period, 45 and 87% for the second period and 20 and 95% for the third period. But independent of the used model, a decrease

in discharge is expected to occur and therefore less water will be available for irrigated agriculture and other sectors. This has to be taken into account for future water management and in the development of new irrigation techniques.

5.3 Impact of land use change on water resources

In figure 5.5 the results of the different land use change scenario's are shown. The dark blue line shows the monthly average discharges simulated, using the land use map op 1984. The lightblue line are the results of the 2013 land use map. The light green line shows the results of an increase in agriculture with 20% decrease in pasture (Future1) and the dark green line the results of 30% decrease in pasture (Future2). The results of the land use change scenario's with a decrease in savanna are shown by the light orange line (20% decrease, Future3) and the orange line (30% decrease, Future4). The red line shows the result for the combined scenario with a decrease in pasture and savanna (Future5).

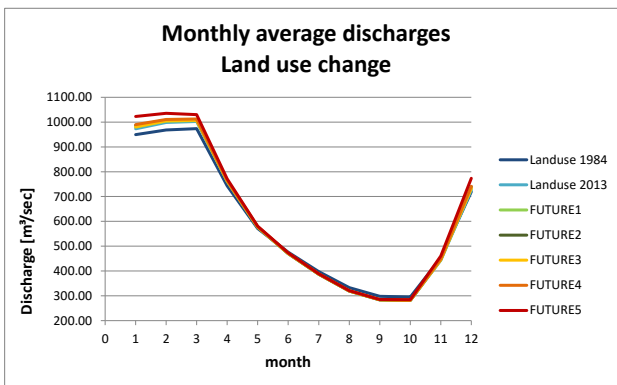


Figure 5.5: Monthly averages for different land use change scenario's at the Porto Alegre station

For all scenario's the change in discharge is very low, compared to the climate change scenario's. In the months of the wet period the discharge increases and during the dry months the discharge decreases. The increase in discharge is highest for the combined land use change scenario (average increase of 42m³/sec) and lowest for the scenario to analyze the change between 1984 and 2013 (average increase of 16m³/sec). The decrease during the dry months is highest for the historical scenario (change from 1984 to 2013 with an average decrease of 11m³/sec) and lowest for the combined scenario with an average decrease of 9m³/sec. Reason for the small changes in discharge due to land use change can be a similarity in transpiration between the crops of savanna resp. pasture and soybean (which is used as representative crop

for rain-fed agriculture). All in all it can be said that land use change, regarding a decrease of pasture and savanna for an increase in agricultural area, have less influence on the available water in the river, compared to a change in climate.

5.4 Impact of irrigation on water resources

In figure 5.6 the results of the irrigation scenarios are shown. The results are the monthly average discharges at the Porto Alegre station. The dark blue line is the case with no irrigation (period 1984/1985) and the lightblue line shows the monthly averages of the scenario with irrigation (period 2010/2011). The average decrease in discharge between 1984 and 2010 is 253m³/sec. This difference was used to determine the decrease in discharge, while increasing the irrigation area.

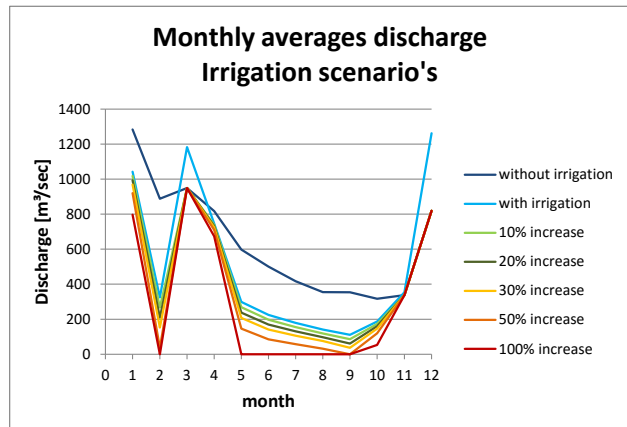


Figure 5.6: Monthly averages for different irrigation scenario's at the Porto Alegre station

The green, orange and red lines show the discharges of the different scenarios. With an increasing area, the discharge decreases continuously. The decrease in discharge is largest between the period of 1984/1985 and 2010/2011, because between these two periods the irrigation area increased by nearly 60 times. When increasing the irrigation area with 50%, the discharge becomes 0 during February and September. For an increase of the irrigated areas with 100% the discharge becomes 0 for February and May to September. This means that if the irrigated areas are increased by 50% or more, the river will be in a critical condition during several months of the year. Thus other sources for irrigation water are needed, when irrigation areas become larger. Another option is to apply a more efficient irrigation method with less water use to prevent tributaries to dry out during the dry period of the year.

6 | Discussion and Conclusion

Within this chapter points of improvement are discussed and recommendations are given for further research. Furthermore the main conclusions of this research are summarized.

6.1 Discussion and Recommendations

6.1.1 Data

The quality of the results highly depends on the quality of the input data. For this research it is assumed that the used data is of good quality. Actually there have been some gaps inside the time series, which have been gapfilled, using other data sources and data of stations close by. The gapfilling by stations close-by can lower the data quality, because of spatial variability between the different stations. For further research it is recommended to find more complete time series or gapfilling methods, that takes the spatial variability into account.

Another point of discussion is the density of meteorological stations inside the project area. Because of spatial variability between the stations, the amount of stations in this research might be too low. Advice for further research is to get data of more stations to have a higher spatial density of climate measurements.

6.1.2 Hydrologic modelling and calibration

Even after the manual calibration of the model, the model still overestimates the discharge, compared to measured values. This has to be taken into account, when using the results for future water management. Furthermore it is recommended to also perform a automatic calibration in addition to the manual calibration. The automatic calibration in combination with the manual calibration might lead to better results of the model performance. Automatic calibration can also be used to show the confidence regions of the model to derive the accuracy of the simulated discharge.

Also the calibration within this research is only executed for one measurement station close to the outflow point of the whole Paracatu River Basin. It is uncertain how the model will perform for individual subbasins. To improve the reliability of model results in sub basins, the calibration should be carried out for several stations inside the PRB.

6.1.3 Climate Change Scenarios

The different used climate models and different used method to correct the time series of the climate models lead to different results. Further research is necessary to determine, which model and correction method lead to the most realistic results.

6.1.4 Land use Change Scenarios

The future land use change scenario's are implemented into the model by using the land use change module in ArcSWAT and using a random raster within ArcGIS. Both methods do not take protected nature areas into account. When these areas are taken into account, the change for savanna into agriculture might only take place in specific regions and might lead to different results. Also the methods lead to a random combination of land use types with specific soil types. When only increasing the areas around current agricultural areas, the combination of land use and soil types might be different and might lead to different results.

Another assumption made in this research is to use soybean as a representative crop for rainfed agriculture. If other crops are used as representative crop or detailed crop maps are used, the results could become differently. The last assumption made with the land use change scenario's is the stationarity of the input parameters (changed during calibration). Actually these parameters could be different for other land uses (e.g. the maximum canopy storage). But this assumption has to be made, because otherwise the results by using different land use maps are not comparable, as changes in discharge could also be caused by changes in these parameters.

6.1.5 Irrigation Scenario's

The main assumption made for the irrigation scenario is that the difference between the discharge of 1984/1985 (without irrigatio) and the discharge of 2010/2011 (with irrigation) is caused by the increase in irrigation only. It is already tested, that precipitation is not of big influence on the change in discharge during the dry period. Actually there could be more causes next to irrigation and a change in precipitation, leading to the difference between those two discharge time series. Furthermore it is assumed that the increase in irrigation area and decrease in discharge have a linear relation.

Actually this relation might not be linear, because there are many factors, which are of influence when applying irrigation, like return flow etc. Another point which is not taken into account in this research, is the irrigation increase in amount of water per area. When the amount of irrigation water per square-meter increases, discharge might decrease with a different rate. Recommended for further research is to get more data about actual irrigation and apply this in the irrigation module of SWAT or other hydrological models. By using an irrigation module within a hydrological model, more insight can be gained about the processes influenced by irrigation and a better relation between increase in irrigation and decrease in discharge can be found.

6.2 Conclusion

The main question of this research is *"What is the impact of climate and land use change on the (surface) water resources of the Paracatu River Basin and how large is the impact of irrigated agriculture?"*. To answer this question a scenario analysis has been executed. Below the main conclusions per subquestion are given.

The highest discharge occurs during the wet period ($1200\text{m}^3/\text{sec}$) and the lowest average discharge occurs during the dry period of the year ($200\text{m}^3/\text{sec}$). The discharge of the Paracatu River highly depends on rainfall, but not only, because the Paracatu River is one of the perennial tributaries of the São-Francisco river. This means that water flows through the Paracatu River the whole year and does not dry out during the dry season.

Climate change leads to less rainfall and extreme rainfall events. Furthermore there is an increase in temperature. These changes lead to a significant decrease in discharge (between 20 and 95%). Thereby the rcp 8.5 scenario's lead to larger decreases in discharge compared to the rcp 4.5 scenarios. Furthermore larger decreases are expected when using the ETA HadGEM2-ES model compared to the ETA-MIROC5 model. The largest absolute decrease takes place in March for most of the cases, just before the end of the rainy season. This might lead to water shortages for irrigation and other sectors during the dry season, who are dependent on the filling of the water reservoirs during the wet season. The change in discharge expected due to climate change is a decrease between 20 and 95%. So independent of the used climate model, a decrease in discharge can be expected for the future and has to be taken into account for future water management.

The land use change, as expected for the study area, is an increase in rainfed and irrigated agriculture with a decrease of savanna and pasture areas. The decreases in discharge due to the land use changes are relatively small, compared to the discharge decrease caused by climate change. The decrease in discharge caused by the increase of irrigation areas is large between 1984/1985 and 2010/2011, because between these two periods the irrigation area increased by approximately 60 times. After increasing the irrigation area of 2013 with 10, 20, 30, 50 and 100%, the discharge decreases continuously. When increasing the area with 50 and 100%, the discharge becomes 0 during some months of the dry period. This means that there is a limit on the increase in irrigation areas. This limit has to be taken into account in future development of the agricultural sector, by developing more efficient irrigation methods and get larger yields on smaller space.

All in all the conclusion is that climate change as well as land use change is expected in the future. Climate change is of bigger influence compared to land use change. Irrigation can have large influence on the water availability, if the increase in irrigated areas will become too large.

Bibliography

- Allen, R. G., Pereira, L. S., Raes, D., Smith, M., 1998. Crop evapotranspiration - Guidelines for computing crop water requirements, FAO Irrigation and drainage paper 56. FAO - Food and Agriculture Organization of the United Nations.
- Aquino, R. F., Silva, M. L. N., Freitas, D. A. F. A. d., Curi, N., Avanzi, J. C., 02 2013. Soil losses from typic cambisols and red latosol as related to three erosive rainfall patterns. *Revista Brasileira de Ciênciortdfe-meninencia do Solo* 37, 213 – 220.
URL http://www.scielo.br/scielo.php?script=sci_arttext&pid=S0100-06832013000100022&nrm=iso
- Arnold, J., Kiniry, J., Srinivasan, R., Williams, J., E.B., H., Neitsch, S., 2012a. Swat input output documentation - version 12.
- Arnold, J., Moriasi, D., Gassmann, P.W., A. K., White, M., Srinivasan, R., Santhi, C., Harmel, R., van Griensven, A., Van Liew, M., Kannan, N., Jha, M., 2012b. Swat:model Use, Calibration, and Validation. American Society of Agricultural and Biological Engineers.
- Bilibio, C., Hensel, O., Selbach, J., 2011. Sustainable water management in the tropics and subtropics and case studies in Brazil, Vol.1. Fundação Universidade Federal do Pampa, UNIKASSEL, PGCUI, UFMA.
- Biswas, A. K., Cordeiro, N. V., Braga, B. P. F., Tortajada, C., 1999. Management of Latin American River Basins: Amazon, Plata, and São Francisco. United Nations University: Water Resources Management and Policy.
- Bjornaes, C., 2015. A guide to representative concentration pathways.
- Bof, L. H. N., Pruski, F. F., da Silva, L. M. C., Justino, F., 2013. Analysis of appropriate timescales for water diversion permits in brazil. *Environmental Management* 51 (2), 492–500.
- Braga, B. P. F., Flecha, R., Thomas, P., Cardoso, W., Coelho, A. C., 2009. Integrated Water Resources Management in a Federative Country: The Case of Brazil. *International Journal of Water Resources Development* 25 (4), 611–628.
- Brito, R., Bastings, I., Bortolozzo, A., 2003. The Paracatu/Entre-Ribeiros Irrigation Scheme in South-eastern Brazil, Features and Challenges in Performance Assessment. *Irrigation and Drainage Systems* 17 (4), 285–303.
URL <http://dx.doi.org/10.1023/B%3AIRRI.0000004565.38120.63>
- Chou, S., Lyra, A., Mourao, C., Dereczynski, C., Pilotto, I., Gomes, J., Bustamante, J., Tavares, P., Silva, A., Rodrigues, D., Campos, D., Chagas, D., Sueiro, G., Siqueira, G., Marengo, J., 2014. Assessment of climate change over south america under rcp 4.5 and 8.5 down-scaling scenarios.
- de Andrade e Santos, H., dos Santos Pompeu, P., Kenji, D., 2012. Changes in the flood regime of São Francisco River (Brazil) from 1940 to 2006. *Regional Environmental Change* 12 (1), 123–132.
URL <http://dx.doi.org/10.1007/s10113-011-0240-y>
- De Oliveira Latuf, M., Martinez, M. A., Pruski, F. F., da Silva, D. D., 2007. Mudanças no uso do solo nas bacias do rio Preto e ribeirão Entre Ribeiros/MG a partir de imagens do sensor Landsat 5 TM. *Anais XIII Simpósio Brasileiro de Sensoriamento Remoto, Florianópolis, Brasil*, 5855–5862.
- dos R. Pereira, D., Martinez, M. A., da Silva, D. D., Pruski, F. F., 2016. Hydrological simulation in a basin of typical tropical climate and soil using the {SWAT} model part i: Calibration and validation tests. *Journal of Hydrology: Regional Studies*.
- FAO, 2016. Aquastat website.
URL http://www.fao.org/nr/water/aquastat/countries_regions/bra/index.stm
- Fujaco, M. A. G., Leite, M. G. P., 2010. Agricultural influence on the hydrogeochemistry of the subbasins of the Verde, Entre Ribeiros and Escuro Rivers of Paracatu Hydrographic Basin (MG) - Brazil. *Management of Environmental Quality: An International Journal* 21 (4), 505–522.
- Garbossa, L. H. P., de Vasconcelos, L. R. C., Lapa, K. R., Blainski, E., Pinheiro, A., 2011. The use and results of the Soil and Water Assessment Tool in Brazil: A review from 1999 until 2010.
- IBGE, 2016. Ibge database.
URL <http://www.ibge.gov.br/home/>
- INPE, 2016. Inpe database.
URL <http://www.inpe.br/>

- IPCC, 2014. Climate change 2014: Synthesis report. contribution of working groups i, ii and iii to the fifth assessment report of the intergovernmental panel on climate change.
- Lau, J., 2016. Introduction to oxisols.
URL http://202.82.16.155/bss/geography/notes/Introduction_to_oxisols_soil.pdf
- Lima, E. d. P., Sedyama, G. C., Silva, B. B. d., Gleriani, J. M., Soares, V. P., 12 2012. Seasonality of net radiation in two sub-basins of paracatu by the use of modis sensor products. *Engenharia Agrícola* 32, 1184 – 1196.
- Lorz, C., Abbt-Braun, G., Bakker, F., Borges, P., Börnick, H., Fortes, L., Frimmel, F. H., Gaffron, A., Hebben, N., Höfer, R., Makeschin, F., Neder, K., Roig, L. H., Steiniger, B., Strauch, M., Walde, D., Weiß, H., Worch, E., Wummel, J., 2012. Challenges of an integrated water resource management for the distrito federal, western central brazil: climate, land-use and water resources. *Environmental Earth Sciences* 65 (5), 1575–1586.
URL <http://dx.doi.org/10.1007/s12665-011-1219-1>
- Mearns, L., Hulme, M., Carter, T., Leemans, R., Lal, M., Whetton, P., 2001. Climate Scenario Development.
- Mello, E. L. d., Oliveira, F. A., Pruski, F. F., Figueiredo, J. C., 12 2008. Efeito das mudancas climaticas na disponibilidade hadrica da bacia hidrografica do Rio Paracatu. *Engenharia Agrícola* 28, 635 – 644.
- Melo, G. L. d., Fernandes, A. L. T., 10 2012. Evaluation of empirical methods to estimate reference evapotranspiration in Uberaba, State of Minas Gerais, Brazil. *Engenharia Agrícola* 32, 875 – 888.
URL http://www.scielo.br/scielo.php?script=sci_arttext&pid=S0100-69162012000500007&nrm=iso
- Mingoti, R., Spadotto, C., MORAES, D., 2015. Determinacao de regioes susceptiveis a contaminacao da agua subterranea em funcao de propriedades dos solos no cerrado brasileiro.
- Moriasi, D. N., Arnold, J. G., Liew, M. W. V., Bingner, R. L., Harmel, R. D., Veith, T. L., 2007. MODEL EVALUATION GUIDELINES FOR SYSTEMATIC QUANTIFICATION OF ACCURACY IN WATERSHED SIMULATIONS.
- Mulholland, D. S., Boaventura, G. R., Araujo, D. F., 2012. Geological and anthropogenic influences on sediment metal composition in the upper Paracatu River Basin, Brazil. *Environmental Earth Sciences* 67 (5), 1307–1317.
- NASA, 2016. Power radiation.
URL <http://power.larc.nasa.gov/>
- Neitsch, S. L., Arnold, J. G., Kiniry, J. R., Williams, J. R., 2011. Soil and Water Assesment Tool, Theoretial Documentation, Version 2009.
- Penalba, O. C., Rivera, J. A., 2013. Future changes in drought characteristics over southern south america projected by a cmip5 multi-model ensemble.
- Pereira, S. B., Pruski, F. F., Silva, D. D. d., Ramos, M. M., 12 2007. Estudo do comportamento hidrológico do Rio São Francisco e seus principais afluentes. *Revista Brasileira de Engenharia Agrícola e Ambiental* 11, 615 – 622.
URL http://www.scielo.br/scielo.php?script=sci_arttext&pid=S1415-43662007000600010&nrm=iso
- Rodriguez, R. D. G., 2004. Metodologia para a estimativa das demandas e disponibilidades hidricas: estudo de caso da bacia do paracatu.
- Rodriguez, R. d. G., Pruski, F. F., Novaes, L. F. d., Ramos, M. M., Silva, D. D. d., Teixeira, A. d. F., 04 2007. Estimativa da demanda de Agua nas Areas irrigadas da bacia do rio Paracatu. *Engenharia Agrícola* 27, 172 – 179.
URL http://www.scielo.br/scielo.php?script=sci_arttext&pid=S0100-69162007000100011&nrm=iso
- Stonestrom, D. A., Scanlon, B. R., Zhang, L., 2009. Introduction to special section on impacts of land use change on water resources. *Water Resources Research* 45 (7).
- Terink, W., Lutz, A. F., Simons, G. W. H., Immerzeel, W. W., Droogers, P., 2015. Sphy v2.0: Spatial processes in hydrology. *Geoscientific Model Development* 8 (7), 2009–2034.
URL <http://www.geosci-model-dev.net/8/2009/2015/>
- Teutschbein, C., Seibert, J., 2012. Bias correction of regional climate model simulations for hydrological climate-change impact studies: Review and evaluation of different methods.
- Van Vuuren, D. P., Edmonds, J., Kainuma, M., Riahi, K., Thomson, A., Hibbard, K., Hurtt, G. C., Kram, T., Krey, V., Lamarque, J.-F., et al., 2011. The representative concentration pathways: an overview. *Climatic change* 109, 5–31.

- Vasconcelos, V. V., Martins Júnior, P. P., Hadad, R. M., 2013. Estimation of flow components by recursive filters: case study of paracatu river basin (SF-7), Brazil.
- White, M., Harmel, R., Arnold, J., Williams, J., 2014. Swat check: A screening tool to assist users in the identification of potential model application problems.
- Winchell, M., Srinivasan, R., di Luzio, M., Arnold, J., 2010. ArcSWAT Interface for SWAT2009, User's Guide.
- Winchell, M., Srinivasan, R., di Luzio, M., Arnold, J., 2013. ArcSWAT Interface for SWAT2012, User's Guide.
- Xavier, A. C., King, C. W., Scanlon, B. R., 2016. Daily gridded meteorological variables in brazil (1980 to 2013). *International Journal of Climatology* 36 (6), 2644–2659.
URL <http://dx.doi.org/10.1002/joc.4518>

A | Report field visit

The study area was visited twice on two different locations. The first visit took place in December 2015 to the Paracatu River close to the city Paracatu. In figure A.1 some impressions of the Paracatu River can be seen. The water at this location was not very clear, which can be caused by sediment in the water. Furthermore the Paracatu River is not straight but has some meanders. The river bank has been covered by vegetation. On the way to the Paracatu River, many agricultural sites were passed with center pivot irrigation. The main crop was soybean. Also some nature areas were passed, with vegetation typical for the Cerrado region.



Figure A.1: Paracatu River

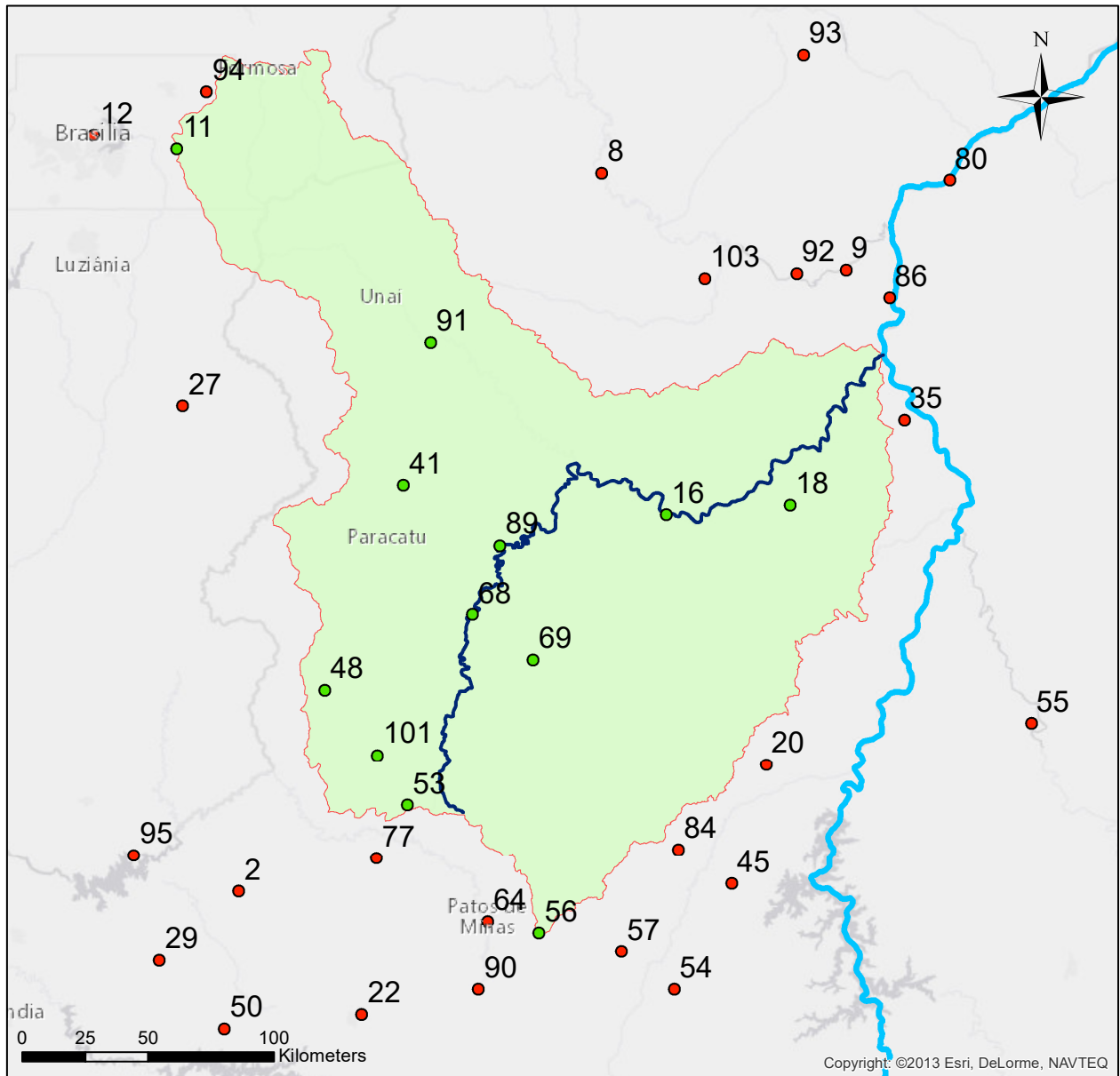
The second field visit took place in January 2016. This time the basin of the Buriti Vermelho River has been visited, a tributary of the Paracatu River. As can be seen in figure A.2 the dimension of the Buriti Vermelho River is much smaller. The basin of the Buriti Vermelho River has been well measured during the last years. During the field visit a new discharge measurement device was installed. When visiting other parts of the basin, some dry tributaries were found, which dried out one year ago. Possible reason could be too extensive use of water within this area.



Figure A.2: Buriti Vermelho River

B | Locations weather and discharge stations

Chosen Rainfall Stations



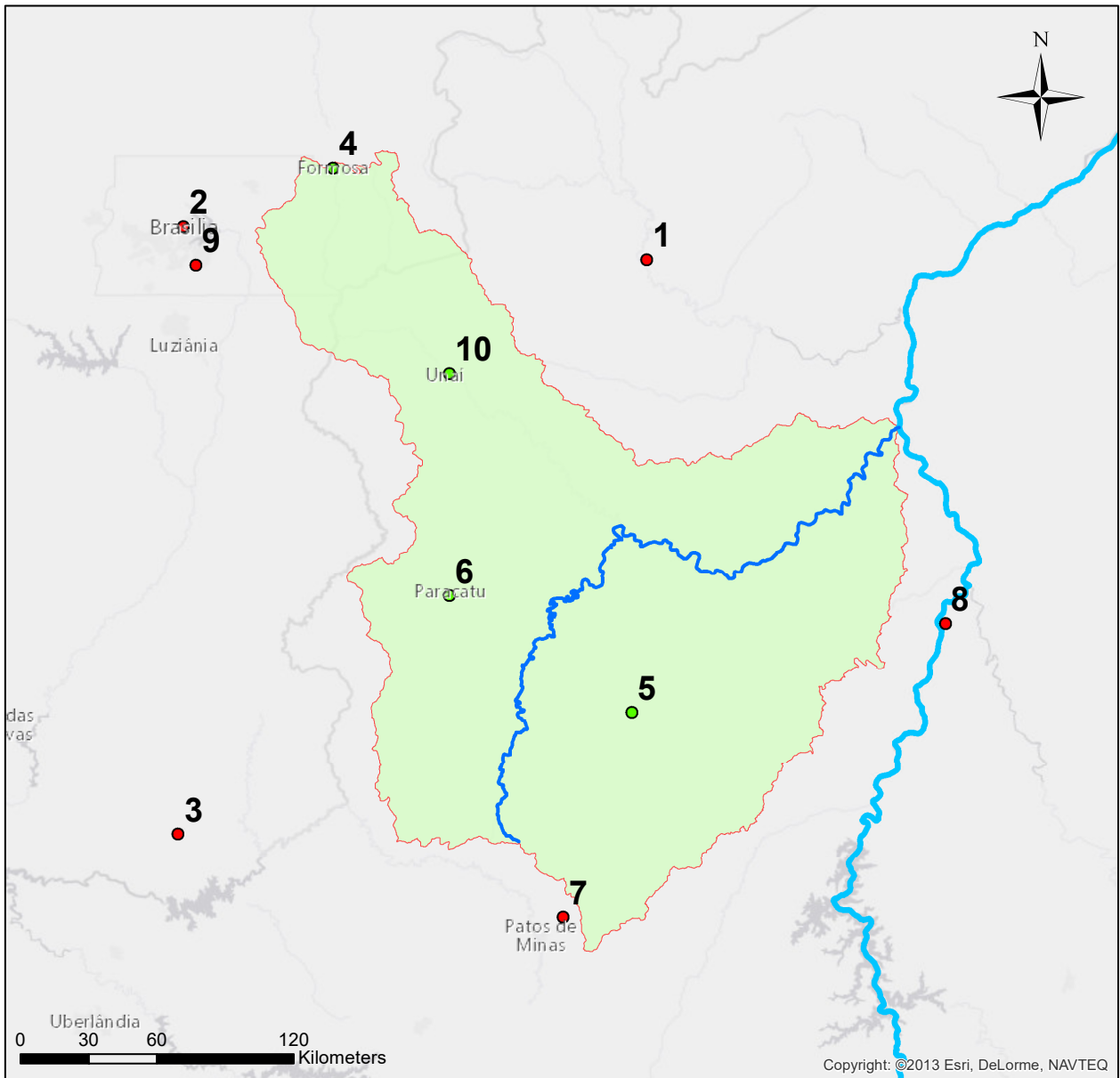
Legend

Stations

- inside basin
- outside basin
- Paracatu River
- São-Francisco River
- Paracatu River Basin

Figure B.1: Locations chosen rainfall stations inside and outside the PRB

Meteorological stations



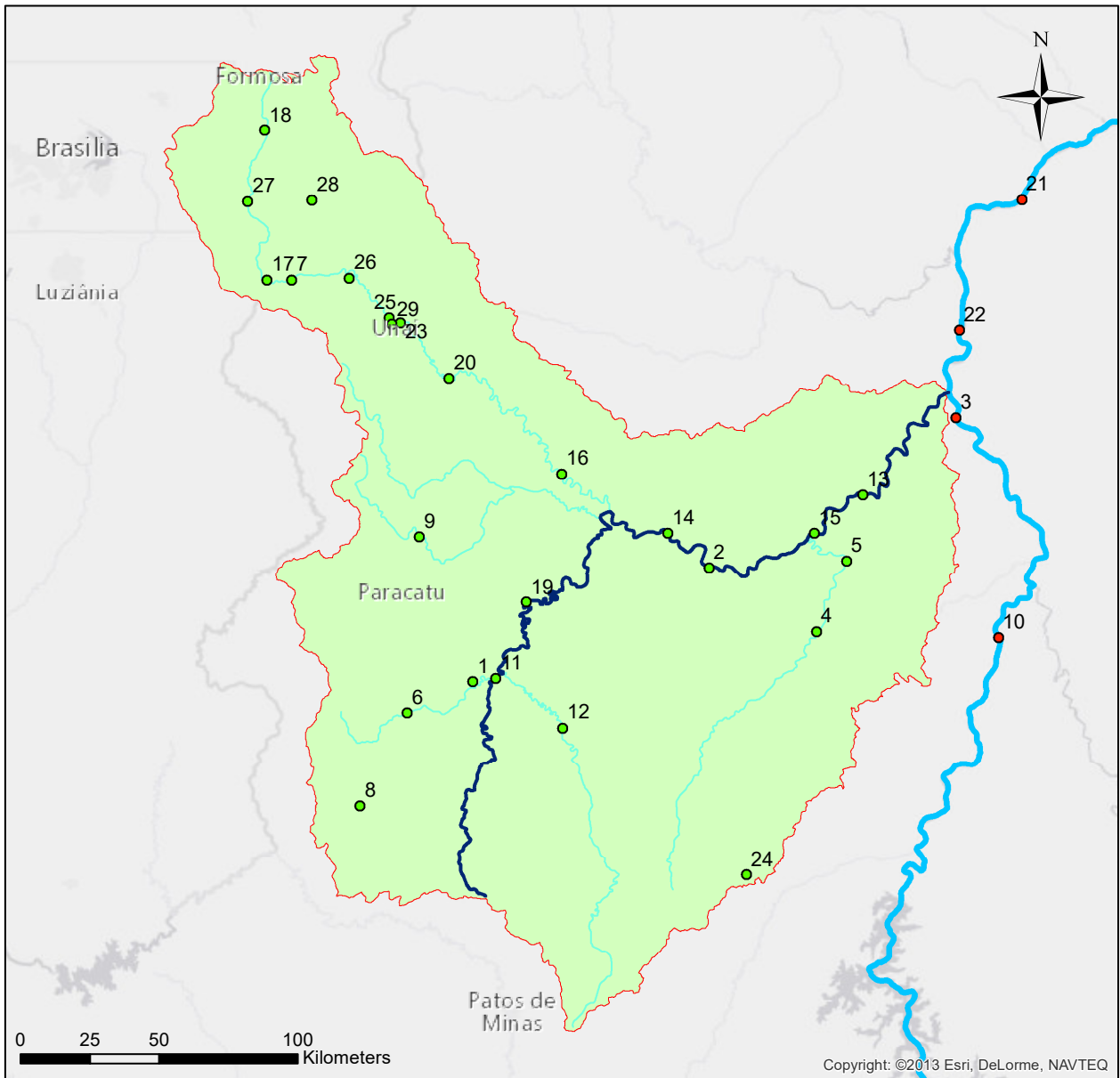
Legend

Stations

- inside basin
- outside basin
- Paracatu River
- São-Francisco River
- Paracatu River Basin

Figure B.2: Locations chosen meteorological stations inside and outside the PRB

Discharge measurement stations



Legend

Stations

- inside basin
- outside basin
- Paracatu River
- Main streams Paracatu
- São-Francisco River
- Paracatu River Basin

Figure B.3: Location discharge stations inside and outside the PRB

C | Data editing

Table C.1: Used data and data sources

Data	Format	Description	Source	Edits
General Data				
Boundary Brazil	Shapefile	Shapefile with the borders of Brazil for creating location map	IBGE - Brazilian Institute of Geography and Statistics	No edits, because this is no model input
States of Brazil	Shapefile	Shapefile with borders and names of Brazilian states for creating location map	IBGE - Brazilian Institute of Geography and Statistics	No edits, because this is no model input
DEM	rasters	digital elevation map of the study area	DEMs of different sources available, chosen for DEM of INPE	The DEM consists of different grid pieces. These pieces are combined within ArcGIS and set into WGS1984 coordinate system
Hydrological data				
Paracatu River Basin	Shapefile	Shapefile with the boundary of the Paracatu River Basin	ANA - National Agency of Water	Transfer the coordinate system and from polygon shape file to grid so that it can be used as mask within SWAT
Preto River Basin	Shapefile	Shapefile with boundary of Preto River Basin	ANA - National Agency of Water	No edits, because this is no model input. Preto River Basin is already included in sub basin file.
Sub basins	Shapefile	Shapefile with boundaries of the sub basins of the Paracatu River.	ANA - National Agency of Water	Names are given per sub basin based on streams flowing through sub basin. Transform coordinate system
São-Francisco River Basin	Shapefile	Shapefile with boundaries of São-Francisco River Basin for creating location map.	ANA - National Agency of Water	No edits, because this is no model input
Paracatu River	Shapefile	Shapefile (line) with the location of the Paracatu River	ANA - National Agency of Water	No edits, because it is no direct model input. Paracatu river will be imported to SWAT by the streams file
Preto River	Shapefile	Shapefile (line) with the location of the Preto River	ANA - National Agency of Water	No edits, because this is no model input
São-Francisco River	Shapefile	Shapefile (line) with the location of the São-Francisco River	ANA - National Agency of Water	No edits, because this is no model input
Streams of the Paracatu River	Shapefile	Shapefile (line) with tributaries of the Paracatu River	ANA - National Agency of Water	Reduce stream file to most important streams and transform coordinate system
Discharge data	Excel files	Excel files of 33 stream gauge stations in- and outside the PRB. Daily average values in m3/sec	ANA - National Agency of Water	Transformation of format to get vertical time series, gapfilling of the time series necessary for this research
Locations stream gauge stations	Shapefile	Shapefile (point) with locations of the stream gauge stations.	EMBRAPA	Created based on the coordinates given by ANA - National Agency of Water. Transformation from point shape file to input table SWAT
Meteorological Data				
Rainfall Data	Excel files	Excel files of 103 stations with daily rainfall values (in mm).	ANA - National Agency of Water	Choose rainfall stations (Timeseries of stations inside basin must begin before 1985 and end between 2007 and 2014, outside basin: begin before 1984 and end between 2013 and 2014; max. 10% missing values), Transformation of format to get vertical time series, Transform to input format of SWAT (one .txt - file per station)
Locations rain fall stations	Shapefile	Shapefile (point) with locations of the rain fall stations.	ANA - National Agency of Water	Created based on the coordinates given by ANA - National Agency of Water, Transform point shape file to input table SWAT
Meteorological data	Excel files	Excel files with either monthly values for averaged maximum and minimum temperature and monthly summed up rainfall or files with daily values of precipitation, maximum and minimum temperature, sun hours, evaporation, relative humidity and wind speed. The first data type is based on data of INMET (National Institute of Meteorology), INPE (National Institute of Space Research), EMBRAPA, ANA (National Water Agency), CEMIG (Minas Gerais Energy Company) and CPRM (Geological Survey of Brazil), the second on data of INMET only. For this research only data of the second type will be used, because it is more complete	INMET, INPE, EMBRAPA, ANA, CEMIG and CPRM	Transformation from sun hours to solar radiation (according to instructions by FAO for determination of solar radiation from measured duration of sunshine incl. assumptions about fraction of extraterrestrial radiation reaching the earth on overcast days, because to less information available for determining other fraction, Allen et al. (1998)). Transformation of format to get vertical time series and gapfilling the data with other data sources and transform to SWAT input format (one .txt - file per station per measured item)
Locations meteorological stations	Shapefile	Shapefile (point) with locations of the meteorological stations.	EMBRAPA	Created based on the coordinates given by INMET - National Institute of Meteorology, transform from point shape file to SWAT input tables
Land use and irrigation				
Irrigation areas	Shapefile	Shapefile with irrigation areas (center pivot irrigation) of the year 2013	ANA - National Agency of Water	used to update land use map
Irrigation areas Preto Basin (past)	Shapefiles	Shapefiles of irrigation areas (center pivot irrigation) within the Preto River basin of every 5 years between 1984 and 2014	EMBRAPA, based on landsat TM5 images	no edits, because it is not necessary as input for the model
Land use maps	Shapefiles	Shapefiles with land use of the years 1984 and 2013	EMBRAPA based on landsat TM 5 images images	Update the 2013 map with irrigation areas. Add water shapes of 2013 to 1984 land use map. Summarize land use classes and change names so both maps are comparable. Transform shape file to grid file, create lookup table to translate land use classes to SWAT
Soil				
Soil map	Shapefile database	and Shapefile with soil types and database with background information	IBGE and Mingoti et. al	Shape file to grid, add soil types to user data base, create lookup table to import soil types to SWAT model

D | Climate change input

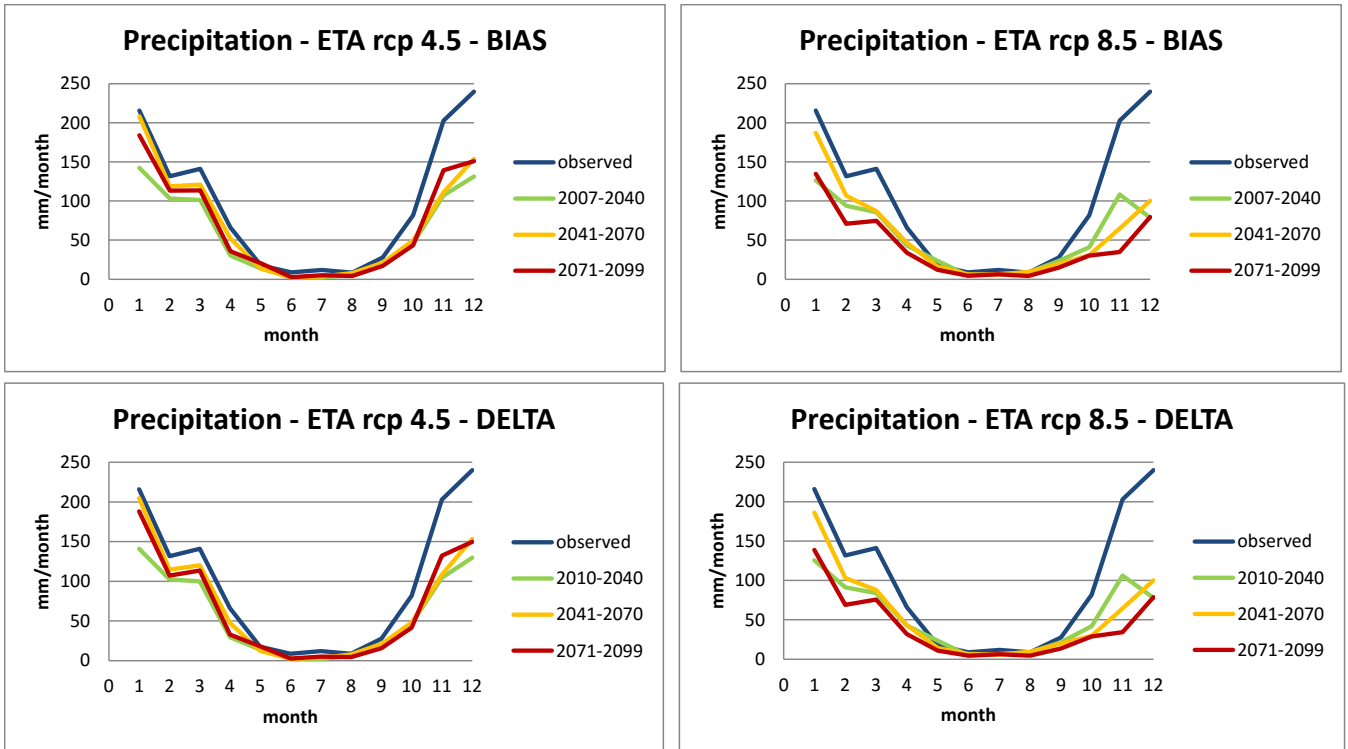


Figure D.1: Climate change input - Precipitation - ETA-model

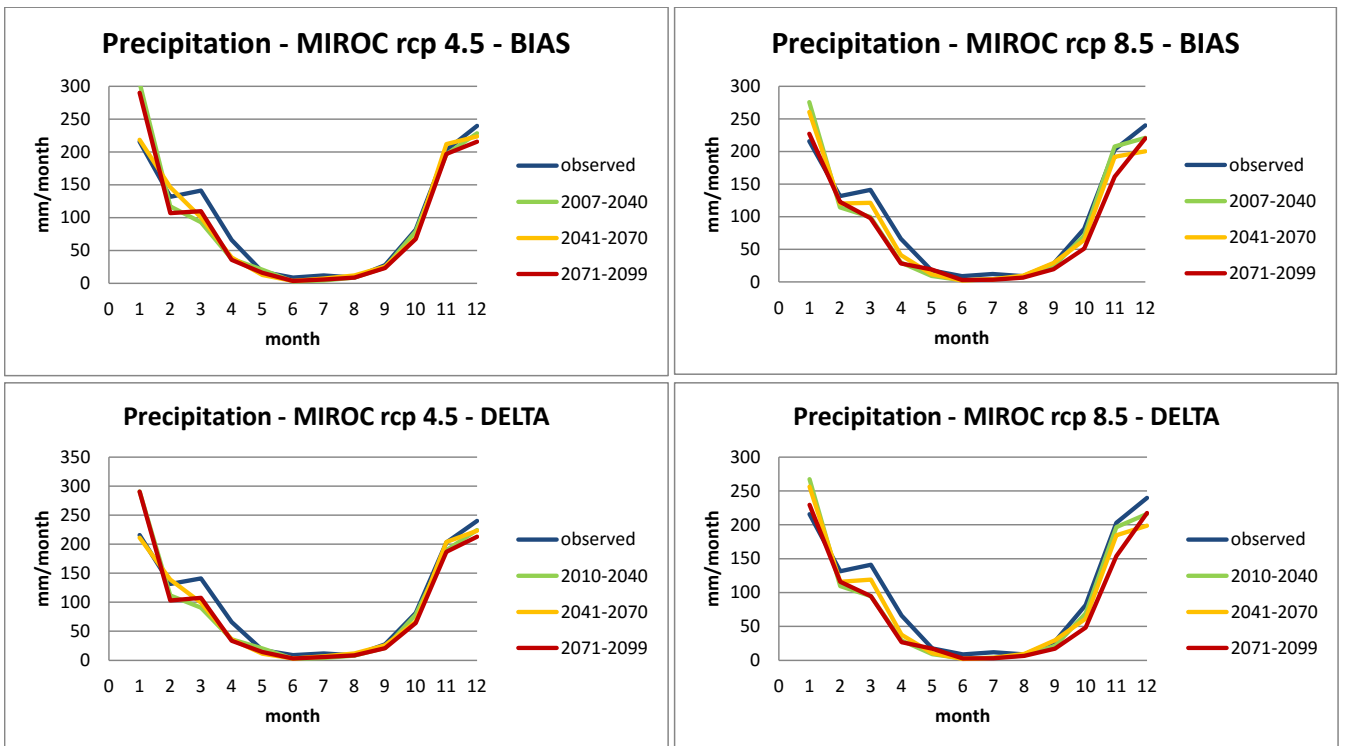


Figure D.2: Climate change input - Precipitation - MIROC-model

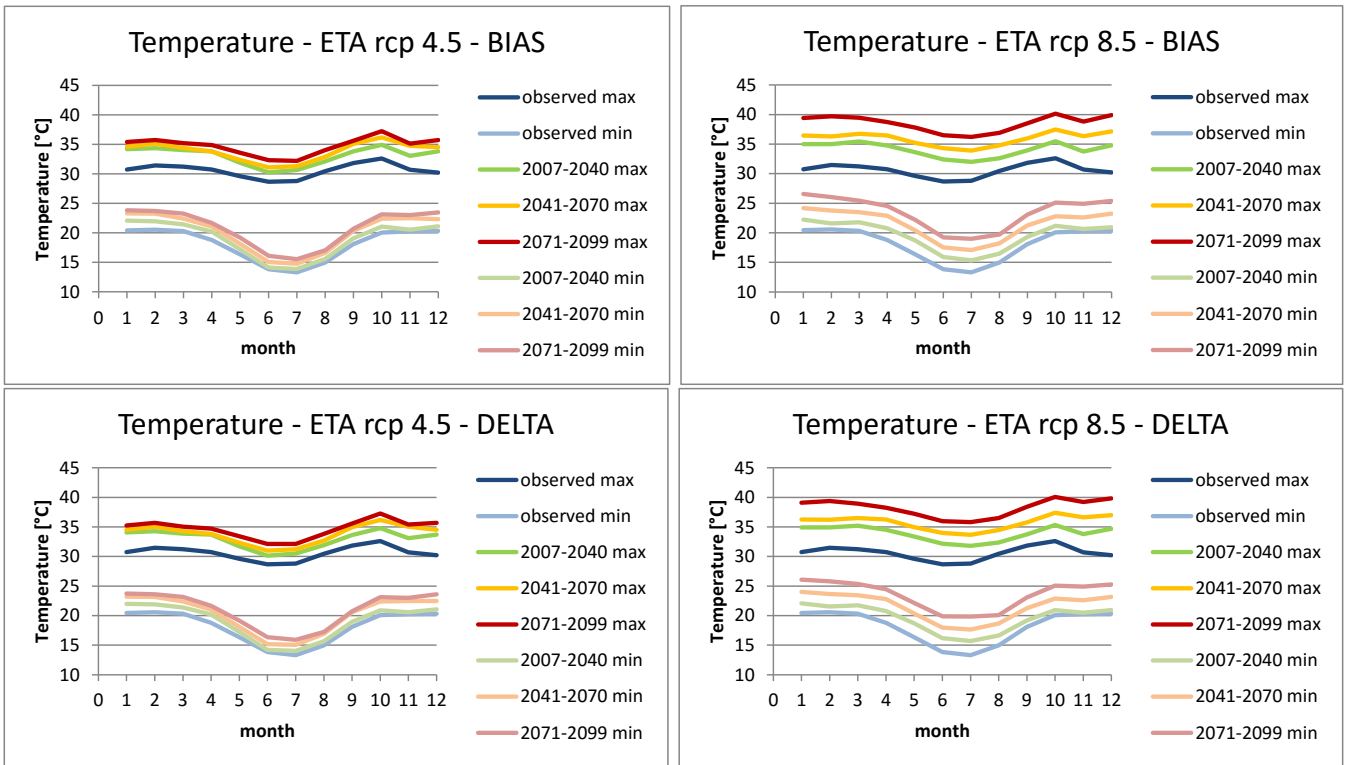


Figure D.3: Climate change input - Temperature - ETA-model

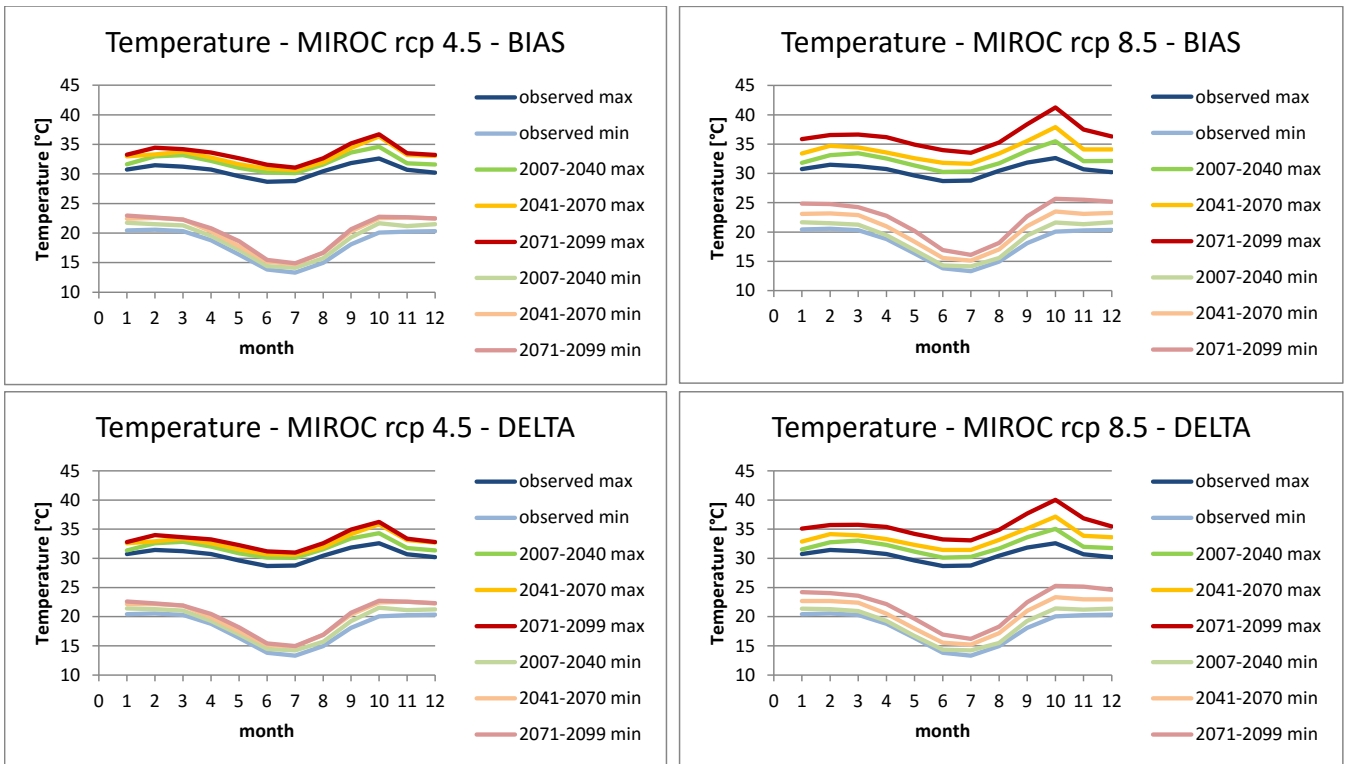


Figure D.4: Climate change input - Temperature - MIROC-model

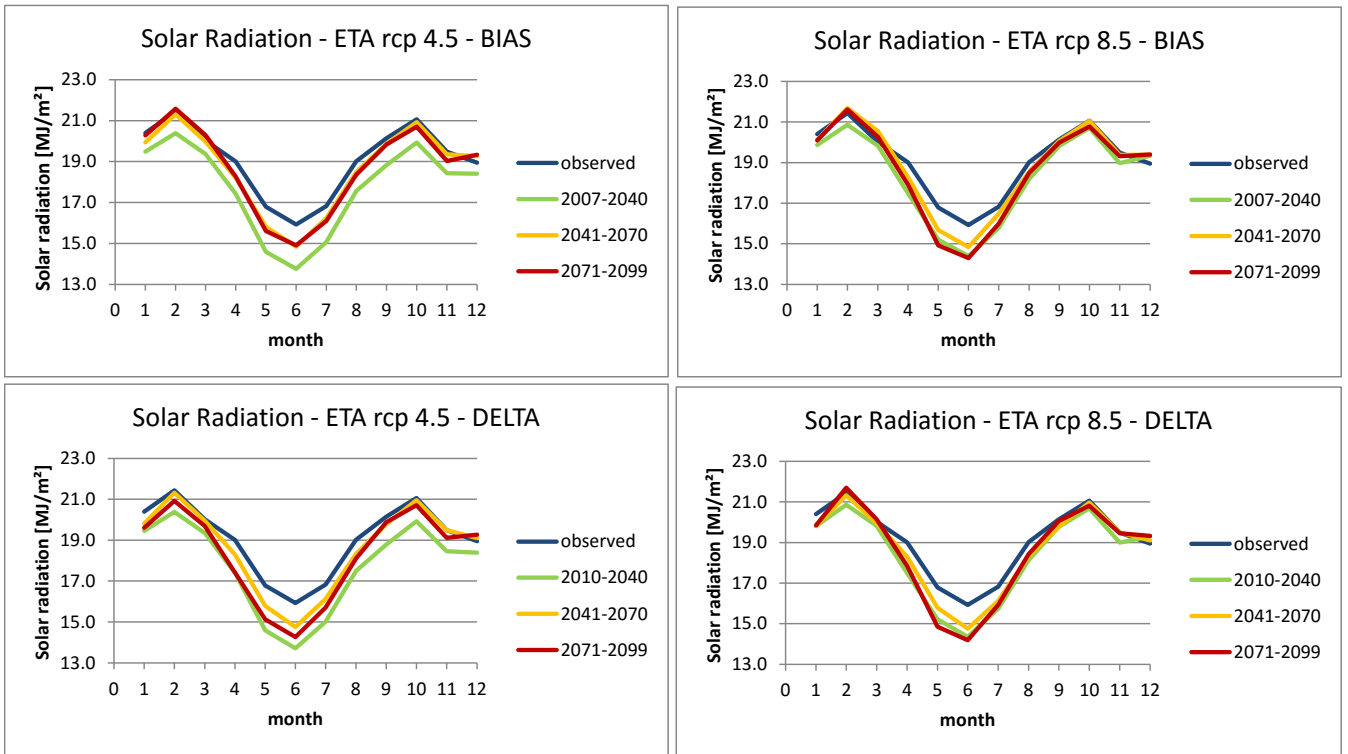


Figure D.5: Climate change input - Solar Radiation - ETA-model

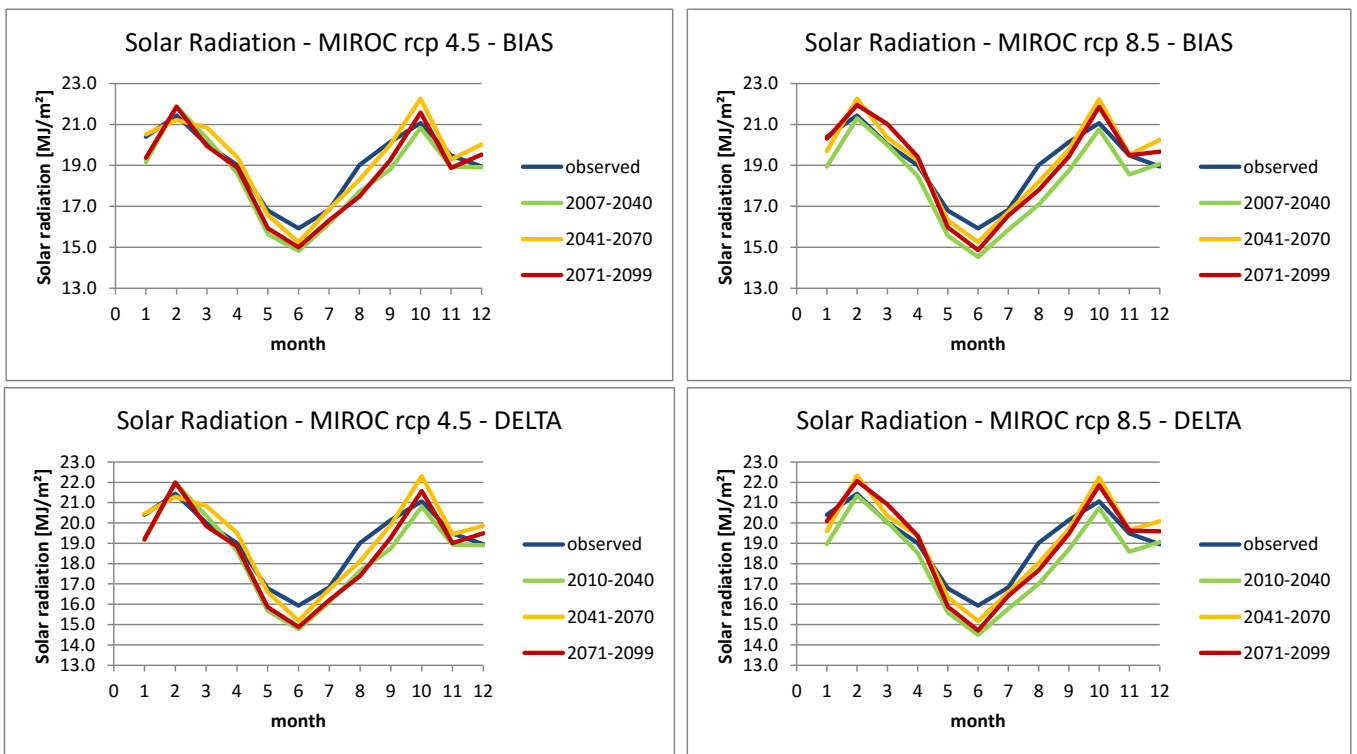


Figure D.6: Climate change input - Solar Radiation - MIROC-model

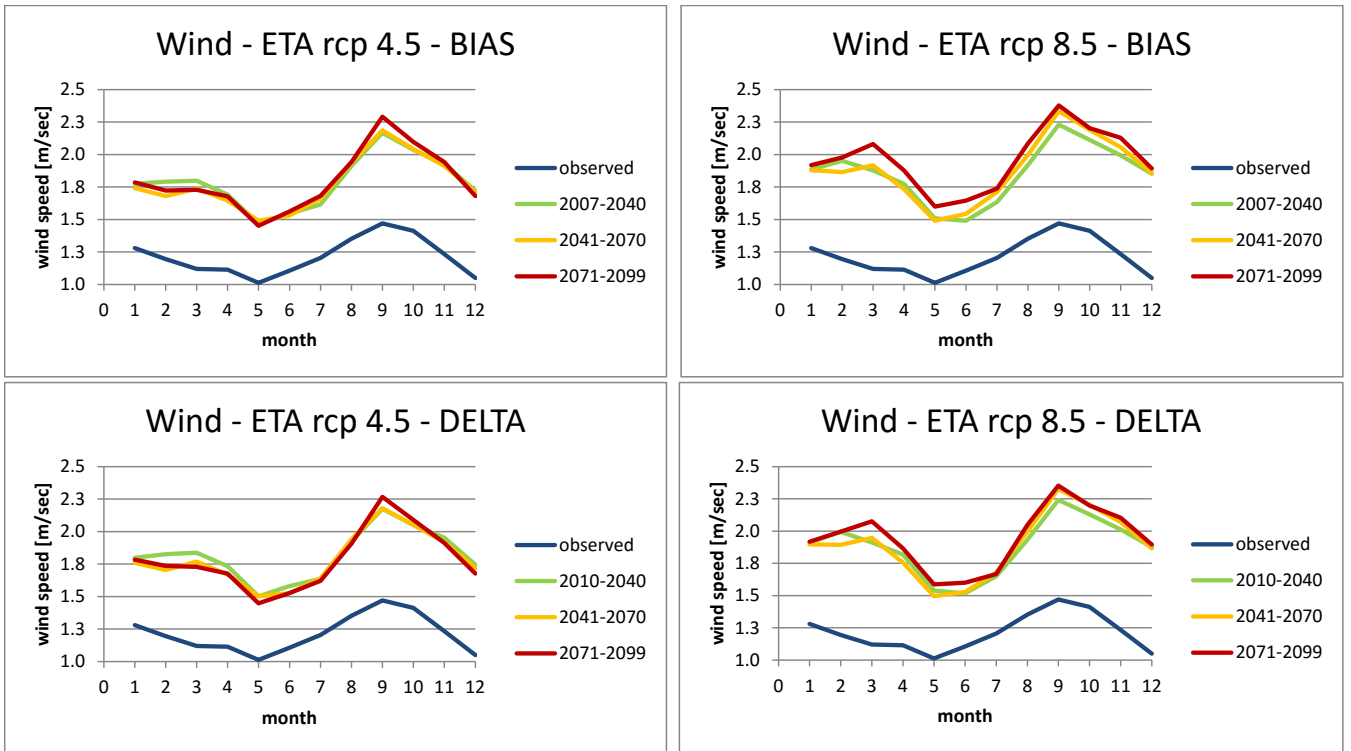


Figure D.7: Climate change input - Wind speed - ETA-model

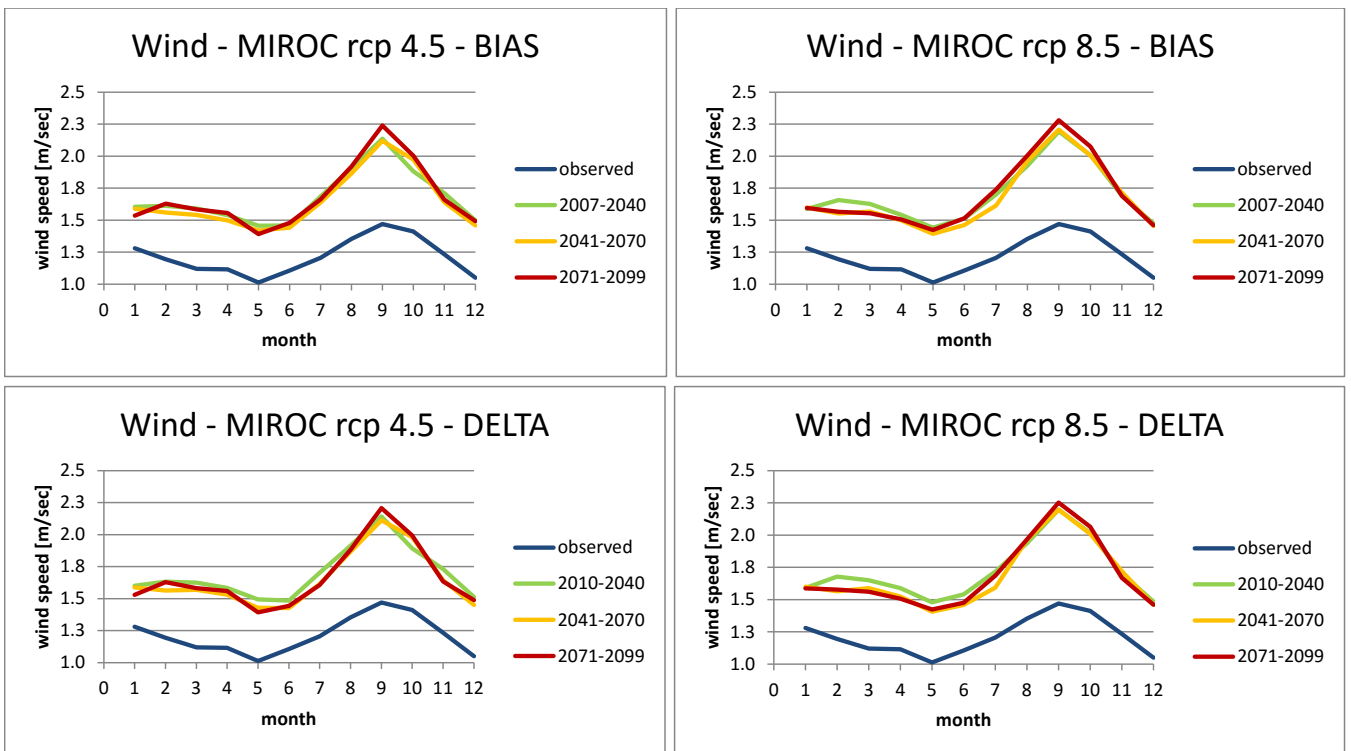


Figure D.8: Climate change input - Wind speed - MIROC-model

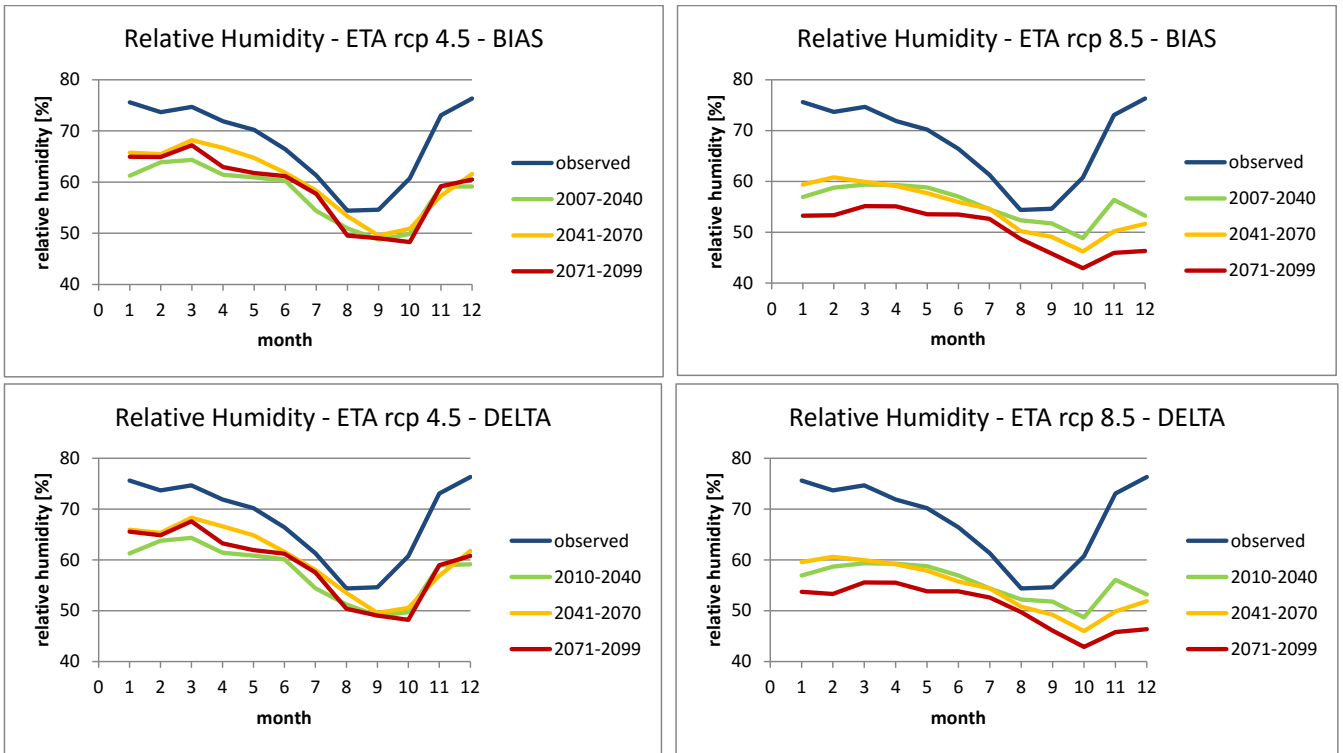


Figure D.9: Climate change input - Relative Humidity - ETA-model

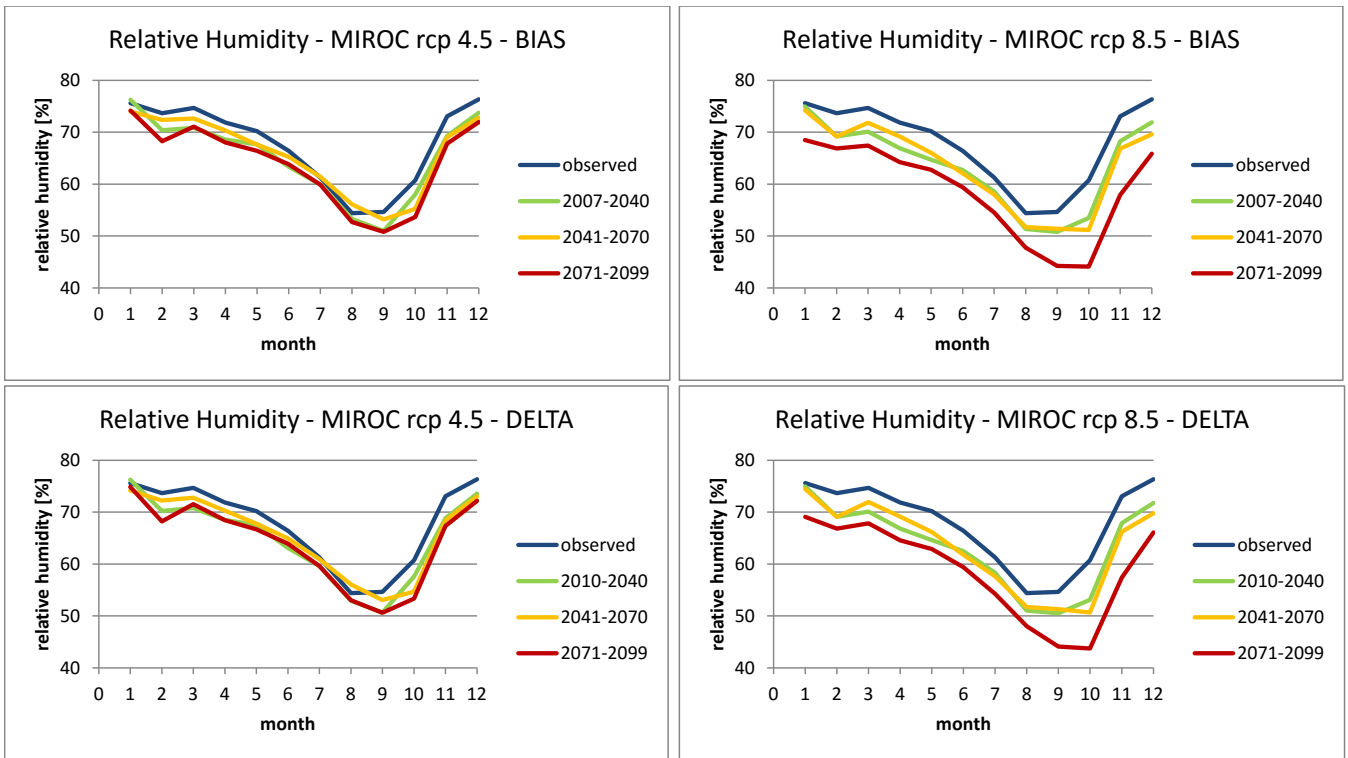


Figure D.10: Climate change input - Relative Humidity - MIROC-model

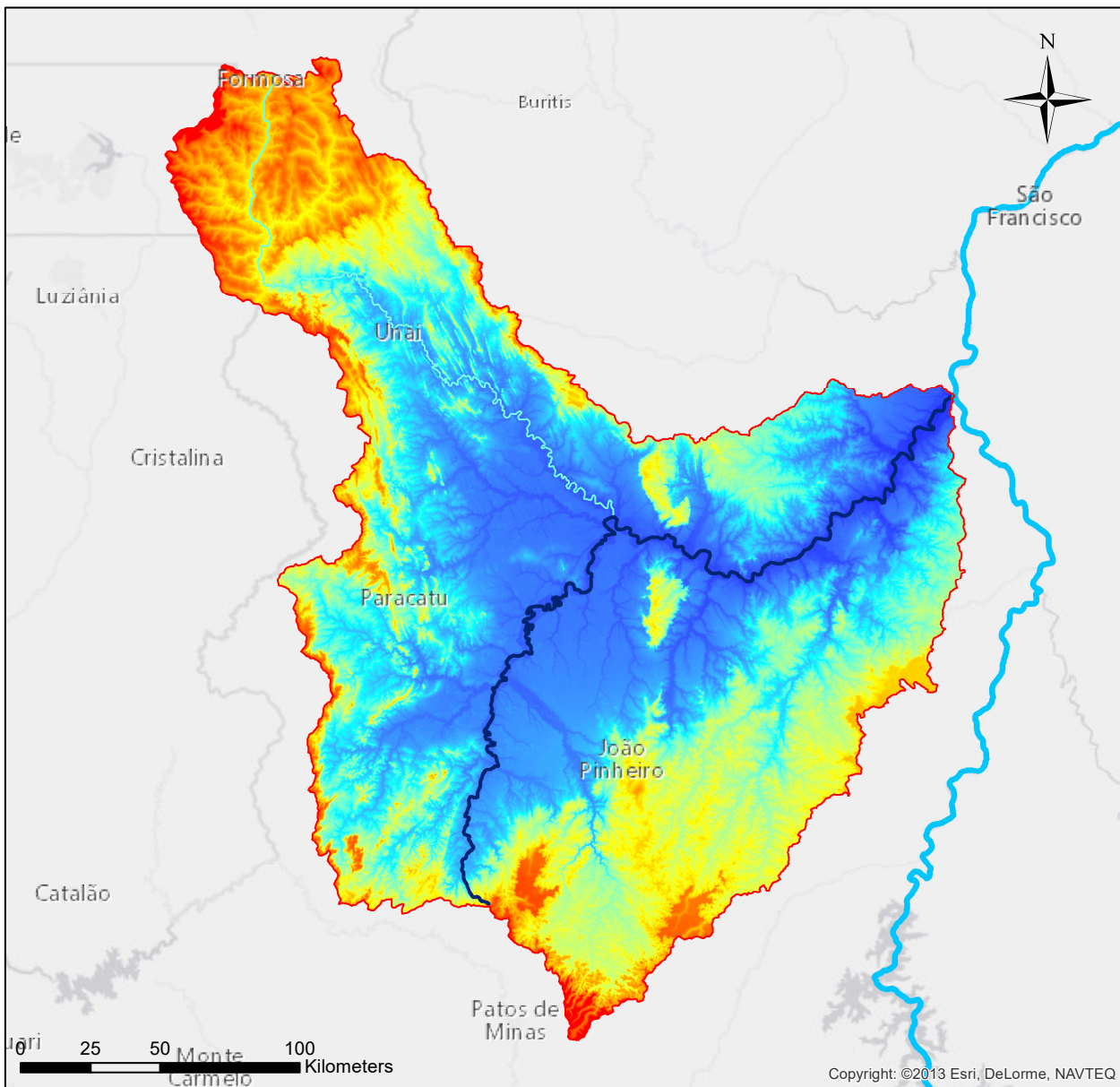
E | Climate change results

Table E.1: Summary results ETA HadGEM2-ES scenario's

	BIAS-correction method rcp4.5			BIAS-correction method rcp8.5			Delta-method rcp4.5			Delta-method rcp8.5		
Period	2007-2040	2041-2070	2071-2099	2007-2040	2041-2070	2071-2099	2007-2040	2041-2070	2071-2099	2007-2040	2041-2070	2071-2099
Average decrease discharge (absolute) (m ³ /sec)	450	329	346	477	494	511	491	420	449	526	513	558
Average decrease discharge (relative) (%)	76	54	58	80	84	87	83	71	76	89	87	95
Months with largest absolute decrease discharge	MAR (744)	MAR (563)	MAR (613)	MAR (811)	MAR (823)	MAR (838)	JAN (794)	JAN (687)	JAN (727)	MAR (865)	MAR (829)	MAR (901)
Months with largest relative decrease discharge	JUN-AUG (78%)	DEC (62%)	MAR (62%)	JAN,JUL,AUG,DEC (82%)	AUG (88%)	NOV (91%)	JUL,AUG (88%)	JUN-AUG (74%)	AUG (81%)	JUL,AUG (93%)	JUL,AUG (91%)	JUN-AUG (98%)
Average decrease precipitation (absolute) (mm/month)	37	24	27	42	39	54	38	26	29	43	40	55
Average decrease precipitation (relative) (%)	43	31	34	31	33	51	44	33	37	33	34	53
Maximum precipitation (mm/day)	90	133	130	82	100	77	102	121	114	110	110	79
Months with largest absolute decrease precipitation	NOV (96mm) DEC (109mm)	NOV (92mm) DEC (86mm)	NOV (64mm) DEC (89mm)	NOV (95mm) DEC (161mm)	NOV (138mm) DEC (139mm)	NOV (168mm) DEC (160mm)	NOV (98mm) DEC (110mm)	NOV (95mm) DEC (87mm)	NOV (71mm) DEC (97mm)	NOV (97mm) DEC (162mm)	NOV (139mm) DEC (140mm)	NOV (169mm) DEC (161mm)
Months with largest relative decrease precipitation	JUN (78%) JUL (83%)	JUN (74%) JUL (71%)	JUN (69%) JUL (56%)	DEC (67%)	OCT (62%) NOV (68%)	NOV (83%)	JUN (77%) JUL (83%)	JUN (74%) JUL (70%)	JUN (72%) JUL (57%)	DEC (68%)	NOV (68%)	NOV (83%)

F | Maps and figures

Digital Elevation Map of the Paracatu River Basin



Legend





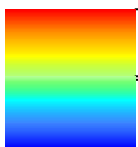
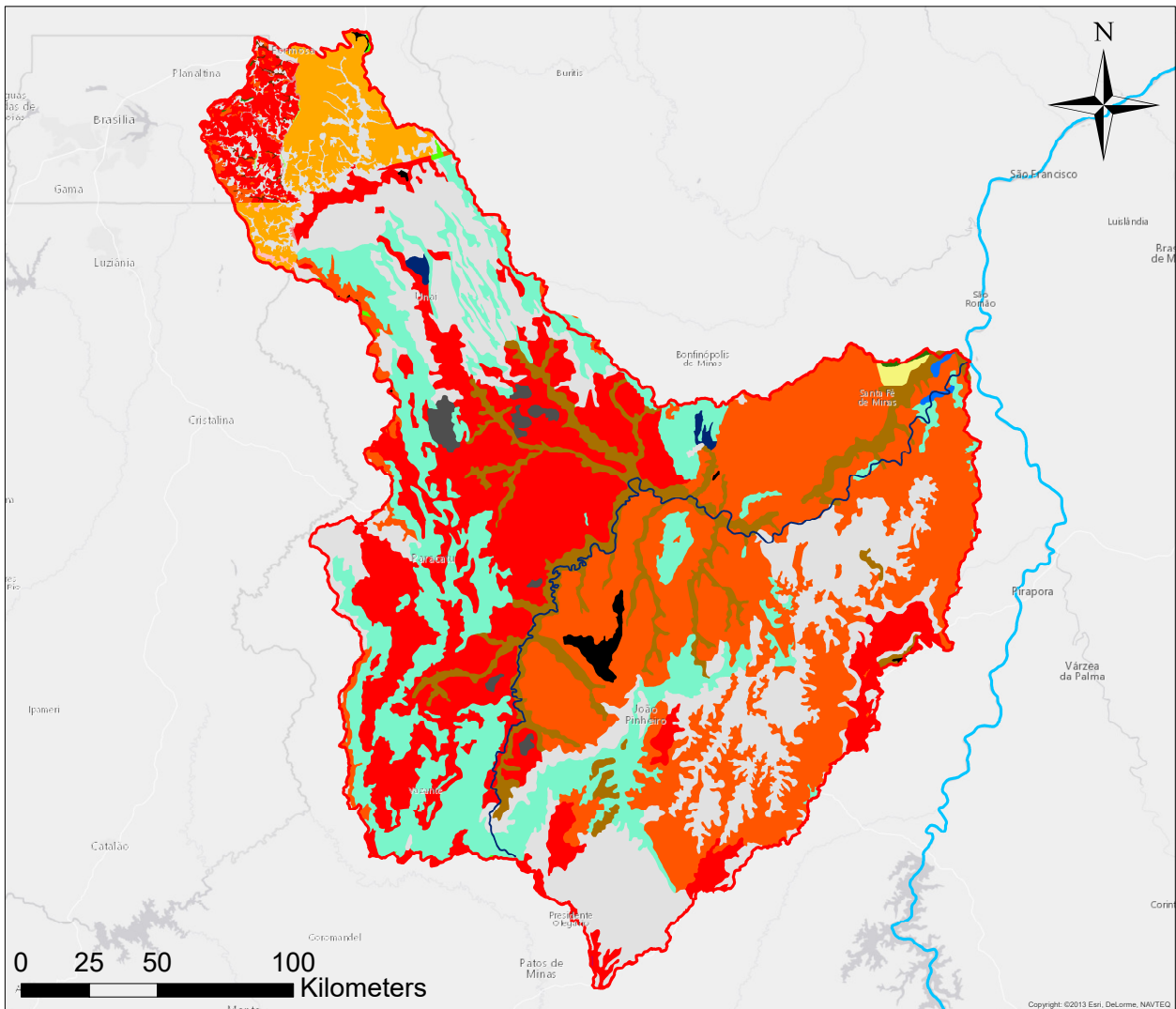
-  Paracatu River Basin
 -  São-Francisco River
 -  Paracatu River
 -  Preto River
-  High : 1192 MASL
Low : 445 MASL

Figure F.1: Digital Elevation Map of the Paracatu River Basin

Soil Map of the Paracatu River Basin



Legend

 Paracatu River Basin	 Red Oxisols (Latosols)	 Plinthosols
 São-Francisco River	 Purple Oxisol (Latosol)	 Hydromorphic indiscriminate soil
 Paracatu River	 Fluvic Neosols	 Red Ultisol
Soil types	 Litholic Neosols	 Gleysol
 Cambisol	 Quartzarenic Neosols	 Quartz sand
 Oxisols (Latosols)	 Stony outcrop	 Lithosol
 Red-Yellow Oxisols (Latosols)	 Petroplinthosols	 Red-Yellow Podzolic
	 Alluvial soil	 Dark-Red Podzolic

Figure F.2: Soilmap of the Paracatu River Basin, based on the soil maps of the IBGE database (IBGE, 2016) and Mingoti et al. (2015).

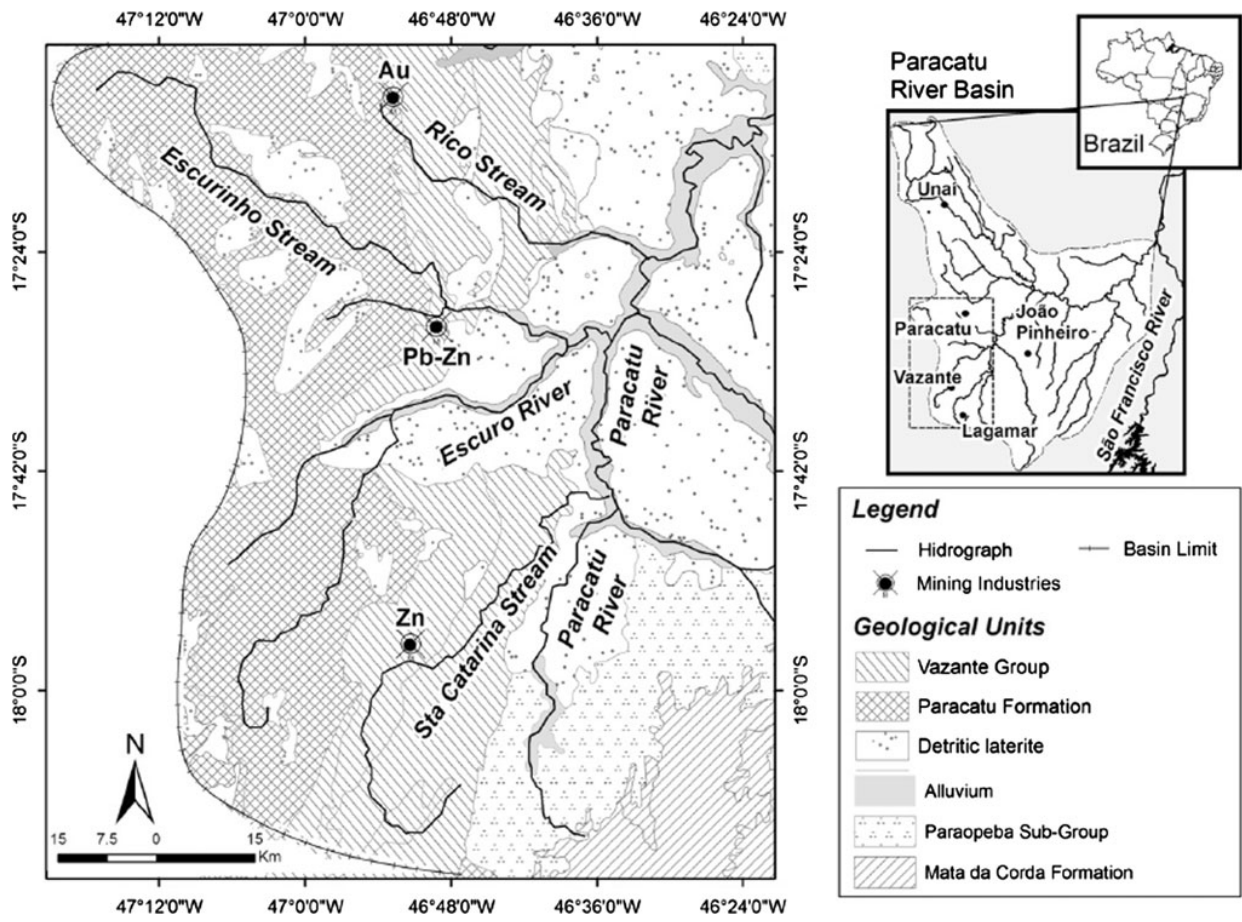
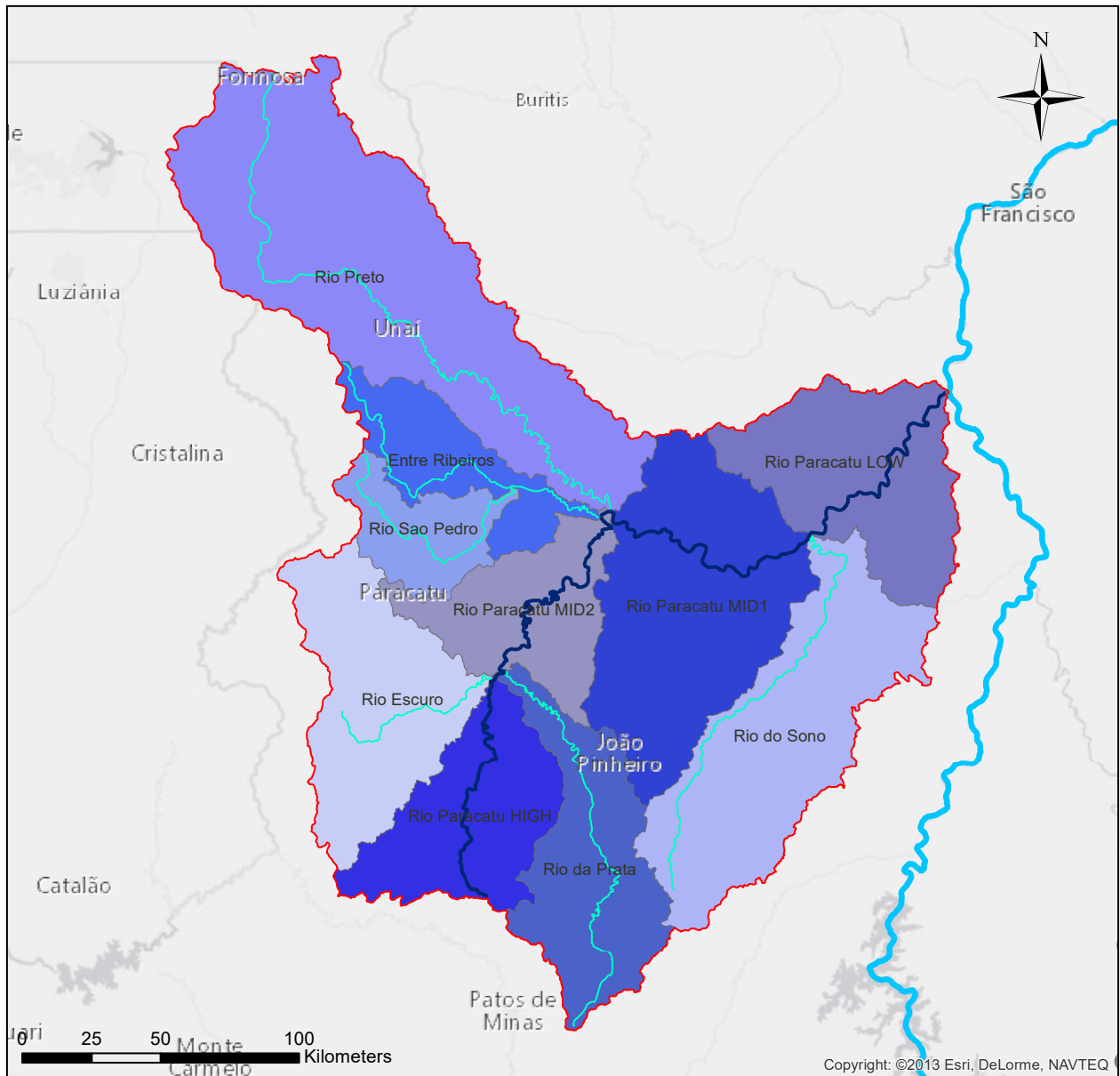


Figure F.3: Main geological units of Upper Paracatu River (Mulholland et al., 2012)

Subbasins and main streams of the PRB

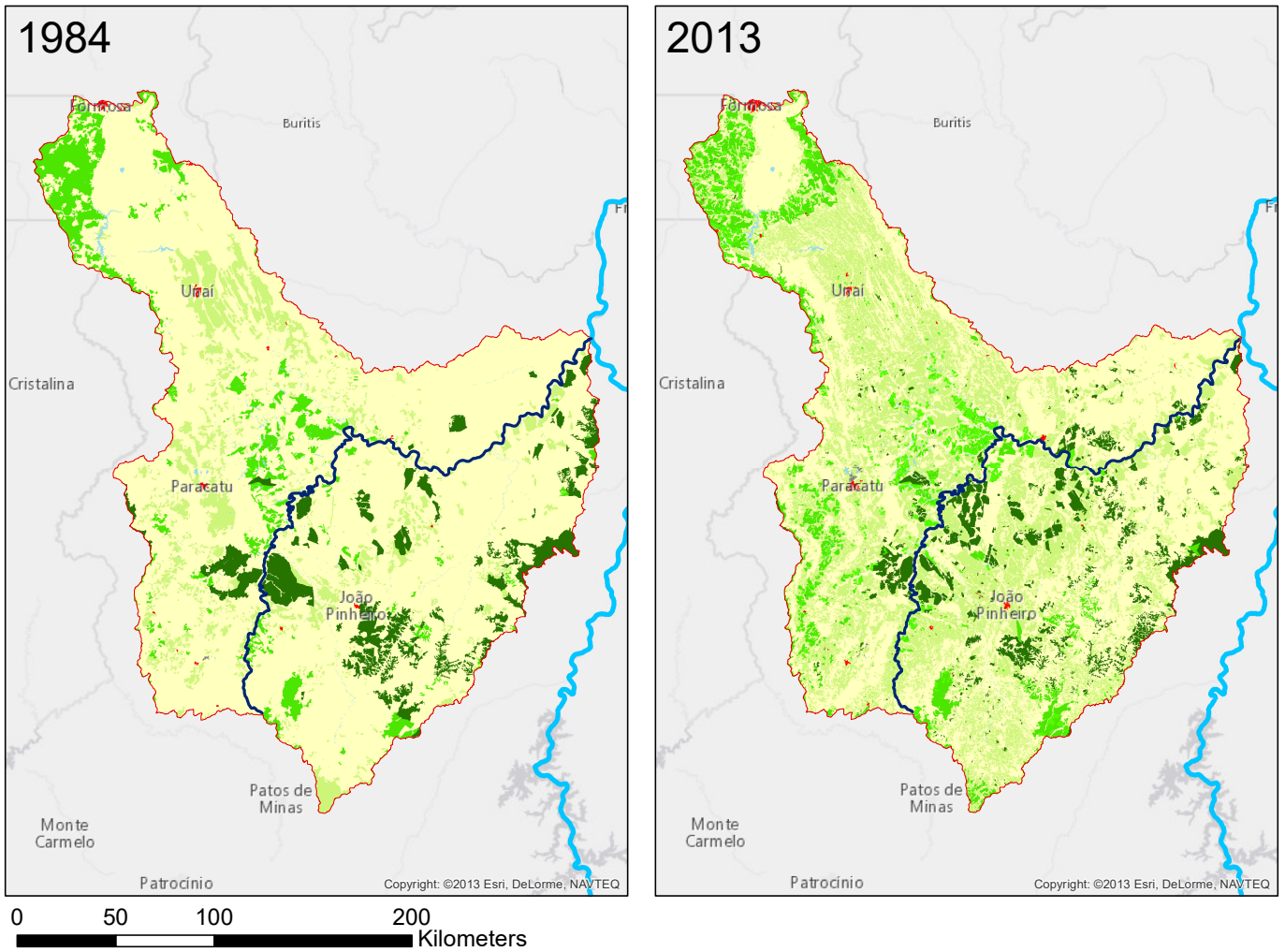


Legend

- Paracatu River Basin
- São-Francisco River
- Paracatu River
- Main streams Paracatu

Figure F.4: Sub basins and main streams of Paracatu River Basin, based on the maps of ANA (National Water Agency) and Rodriguez (2004)

Land use change from 1984 to 2013



Legend

- | | | | |
|--|---|---|---|
|  Paracatu River |  Rainfed Agriculture |  Mining Industry |  Savannah |
|  São-Francisco River |  Irrigated Agriculture |  Pasture |  Water |
|  Paracatu River Basin |  Urban Areas |  Forest | |

Figure F.5: Landuse change of the past 30 years

Development of Irrigation (Center-pivot)

Preto River Basin from 1984 to 2014

